Primary Production in the Southern Ocean, 1997-2006

Kevin R. Arrigo, Gert L. van Dijken, and Seth Bushinsky
Department of Environmental Earth System Science, Stanford University, Stanford, CA 94305

Abstract

Estimates of primary production in the Southern Ocean are difficult to obtain but are essential if we are to understand its role in the global carbon cycle. Here we present a nine-year time series of daily primary production calculated from remotely sensed ocean color, sea surface temperature, and sea ice concentration using a primary production algorithm parameterized specifically for use in Southern Ocean waters. Results suggest that total annual production in waters south of 50°S averaged 1949±70.1 Tg C yr^{-1} between 1998 and 2006, approximately half that of previous estimates. The large but relatively unproductive pelagic province accounted for ~90% of Southern Ocean production, while area-normalized rates of production were greatest on the much smaller continental shelf (109 g C m^{-2} yr^{-1}). Surprisingly, production in the marginal ice zone was only slightly higher than in the pelagic province. The Ross Sea was the most productive sector of the Southern Ocean (mean=503 Tg C yr^{-1}), followed closely by the Weddell Sea (mean=477 Tg C yr^{-1}). Unlike the Arctic Ocean, there was no secular trend in either sea ice cover or annual primary production in the Southern Ocean during our nine-year study. Interannual variability in annual production was most closely tied to changes in sea ice cover, although changes in sea surface temperature also played a role. Only 31% of the variation in annual production was explained by the Southern Annular Mode. Annual primary production could increase in the future as stronger winds increase nutrient upwelling.

1. Introduction

The polar Southern Ocean (waters south of 50°S) is a critical component of global ocean circulation and the biogeochemical cycles of nutrients and carbon. Despite the fact that it represents only 10% of total ocean surface area, it accounts for approximately 25% of the oceanic uptake of atmospheric CO_2 [*Takahashi et al*., 2002]. Much of this CO_2 sink has been attributed to cooling of southward flowing subtropical surface waters and the associated increase in CO_2 solubility (i.e., the solubility pump). Some of the highest concentrations and deepest penetration of anthropogenic carbon are found in the Southern Ocean [*Lo Monaco et al*., 2005; *Waugh et al*., 2006], particularly in the northward moving Antarctic Bottom Water [*Sabine et al*., 2002]. Because these bottom waters were recently in contact with the atmosphere, they are an important water mass for the storage of anthropogenic CO_2 in the deep ocean [*McNeil et al*., 2001].

Another key mechanism that facilitates the influx of atmospheric CO_2 into the Southern Ocean is the biological pump, whereby phytoplankton photosynthesis reduces the surface water partial pressure of CO_2 (pCO_2), creating a gradient between the ocean and atmosphere. When this newly fixed organic carbon sinks out of the upper mixed layer, it may be stored within the deep ocean circulation system for hundreds of years [*Broecker*, 1991]. Hence, Southern Ocean regions with high rates of phytoplankton primary production and an active biological pump are important sites mediating the ocean-atmosphere exchange of CO_2.

On average, the Southern Ocean is characterized by its abundant macronutrients coupled with only modest rates of annual average net primary production [*Arrigo et al*., 1998a; *Moore and Abbott*, 2000]. Despite the generally low phytoplankton abundance, intense phytoplankton blooms occasionally develop, making productivity in the Southern Ocean highly variable both temporally and spatially. The lowest rates of production are generally associated with pelagic waters north of the sea ice zone (SIZ), where rates range from 0.08-0.22 g C m^{-2} d^{-1} in June to 0.5-1.0 g C m^{-2} d^{-1} in December [*Arrigo et al*., 1998a]. Low production rates in these waters are the result of a variety of factors, including low sun angles, deep mixing of the upper water column, and trace metal limitation [*Martin*, 1990; *Mitchell and Holm-Hansen*, 1991, *Boyd et al*., 2000]. One exception to the usually low rates of production characterizing waters north of the SIZ are found along oceanographic fronts, such as the Antarctic Polar Front, where divergence of surface waters brings waters with high nutrient concentrations to the surface, fueling enhanced phytoplankton growth [*Moore and Abbott*, 2000, *Hense et al.,* 2000]. Another exception is found near offshore islands (e.g., the Balleny Islands, South Georgia Island), where current flow past rough or shallowing topography also can increase the flux of nutrients into surface waters [*Korb and Whitehouse*, 2004].

The highest rates of primary production in the Southern Ocean are generally associated with coastal polynyas (regions of open water surrounded by sea ice) [*Arrigo and Van Dijken*, 2003; *Arrigo and Van Dijken*, 2007], the marginal ice zone (MIZ) [*Smith and Nelson*, 1986], and the continental shelf [*Smith and Gordon*, 1997; *Sweeney*, 2003; *Arrigo and Van Dijken*, 2004]. In these environments, rates of CO_2 fixation frequently exceed 2 g C m^{-2} d^{-1}, sufficient to maintain a positive CO_2 gradient between the ocean surface and the atmosphere, facilitating the influx of atmospheric CO_2 [e.g., *Louanchi et al*., 1999a; *Louanchi et al*., 1999b; *Sweeney*, 2003].

Much of what is currently known about large-scale patterns in primary productivity of the Southern Ocean comes from a small number of studies using either satellite-based methods [*Arrigo et al*., 1998a; *Moore and Abbott*, 2000; *Gabric et al*., 2002; *Lovenduski and Gruber*, 2005; *Carr et al*., 2006] or numerical models [*Fennel et al.,* 2003; *Sarmiento et al*., 2004]. However, for a variety of different reasons, these studies have been limited in their ability to assess the spatial variability in Southern Ocean primary production over both short (weekly) and long (interannual) timescales. Here we present an analysis of a nearly decade-long time series of primary productivity determined from space-based measurements of sea ice distribution, sea surface temperature, and chlorophyll *a* (Chl *a*) concentration, together with estimates of mixed layer depth, cloud cover, and spectral irradiance. The algorithm used here to estimate depth-integrated primary productivity is a modified version of that presented in *Arrigo et al.* [1998a]. The current algorithm has been more rigorously validated and benefits from the far superior spatial and temporal Chl *a* coverage afforded by the Sea-viewing Wide Field of view Sensor compared to the Coastal Zone Color Scanner (CZCS). The primary goal of this study was to quantify spatial variability and interannual changes in primary production within the Southern

Ocean and relate the observed patterns to concurrent variability in environmental forcing and climate state (e.g., the Southern Annular Mode, SAM).

2. Methods

2.1. Primary Production Algorithm

The algorithm (modified from *Arrigo et al.*, 1998a) calculates the rate of primary production (mg C m^{-3} hr^{-1}) as a function of diurnal changes in spectral downwelling irradiance, sea surface temperature (°C), and Chl *a* concentration (mg m^{-3}). Horizontal distributions of Chl *a* were determined from 8-day mean SeaWiFS imagery (4 km resolution) for the period 1997 to 2006. We assume that Chl *a* concentration is uniform within the upper mixed layer and decreases exponentially at greater depths, according to the relationship

$$\text{Chl } a(z) = \text{Chl } a(0) \exp[0.033\ (z - \text{MLD})] \quad (1)$$

where z is depth, Chl $a(0)$ is the surface Chl *a* concentration determined from SeaWiFS data, and MLD is the depth of the mixed layer. This relationship was determined using a large number of vertical Chl *a* profiles from the Southern Ocean [*Arrigo et al.*, 2000]. Because waters below the mixed layer account for a small fraction of depth-integrated primary production, the algorithm is relatively insensitive to this parameterization. Primary productivity at each SeaWiFS pixel location is integrated over depth (0-100 m at 1 m intervals) and time (hourly for 24 hours) to determine daily primary production (mg C m^{-2} d^{-1}).

The radiative transfer model of *Gregg and Carder* [1990] is used to compute clear sky downwelling irradiance (E_{dclear}) at hour t which is subsequently corrected for fractional cloud cover (N) according to the equation of *Dobson and Smith* [1988]

$$E_d(\lambda,t)= E_{dclear}(\lambda,t)\ [1 - 0.53(N^{0.5})]. \quad (2)$$

where E_d is the cloud corrected downwelling irradiance, λ is wavelength (nm) and values for N are based on NCEP/NCAR daily reanalysis data [*Kalnay et al.*, 1996]. Other inputs to the radiative transfer model (sea level pressure, wind speed, precipitable water, air temperature, and specific humidity) are also from the NCEP/NCAR Reanalysis project, except for ozone (NASA's Total Ozone Mapping Spectrometer project).

Irradiance is propagated through the water column according to the equation

$$E_d(\lambda,z,t) = (1 - R)\, E_d(\lambda,t) \exp[-K_d(\lambda)\, z] \tag{3}$$

where z is depth (m), and R is the surface reflection [*McClain et al.*, 1996] and

$$K_d(\lambda) = \frac{a_w(\lambda) + a_d(\lambda) + a_s(\lambda) + a^*_{ph}(\lambda) Chl\ a + b_{bw}(\lambda) + b_{bp}(\lambda)}{\mu} \tag{4}$$

where μ is the mean cosine of the angular irradiance distribution, a is absorption, a^*_{ph} is the Chl a-specific absorption by phytoplankton from *Arrigo et al.*, [1998b], and b_b is backscatter. The subscripts w and p represent contributions by seawater and particles, respectively. The inherent optical properties a_w, b_{bw} and b_{bp} are obtained from *Pope and Fry* [1997] and *Smith and Baker* [1981]. Using data from the Ross Sea [*Arrigo et al.*, 1998b], detrital absorption is assumed to vary spectrally and as a function of Chl a concentration according to the equation

$$a_d(\lambda) = 0.006 \text{ Chl } a * \exp(-0.0143(\lambda - 400)) \tag{5}$$

and soluble absorption by CDOM is estimated by

$$a_s(\lambda) = 0.025 \exp(-0.012(\lambda - 400)). \tag{6}$$

Daily primary production (PP, mg C m^{-2} d^{-1}) integrated over the upper 100 m is calculated as

$$PP = \int_{z=0}^{100} \int_{hour=0}^{24} Chla(z) \frac{C}{Chla} G(z,t)\, dz\, dt \tag{7}$$

where $Chla(z)$ is the Chl a concentration at depth z, C/$Chla$ is the phytoplankton carbon to Chl a ratio (88.5 g:g), and $G(z,t)$ is the net biomass-specific growth rate (hr^{-1}) at a given time t and depth z.

G is calculated as a product of the temperature-dependent upper limit to net phytoplankton growth rate, G_{max} (hr^{-1}) and the irradiance limitation term, L (dimensionless), such that

$$G(z,t) = G_{max}(t)\, L(z,t). \quad (8)$$

$G_{max}(t)$ is calculated according to the equation

$$G_{max}(t) = G_O \exp[rT(t)] \quad (9)$$

where G_O is the phytoplankton net growth rate at 0°C (0.59 d^{-1}) and r is a rate constant (0.0633 °C^{-1}) that determines the sensitivity of G_{max} to temperature, T (°C) [*Eppley*, 1972]. The sea surface temperature at time t is obtained from version 2 of the NOAA optimum interpolation sea surface temperature, OISST V2 [*Reynolds et al.*, 2002], and assumed to be constant with depth. While not strictly true, depth-dependent variability in T in the upper ocean tends to be small in polar waters so the impact of this assumption is relatively minor.

The light limitation term, $L(z,t)$, is calculated for each depth and each time step as

$$L(z,t) = 1 - \exp\left(-\frac{PUR(z,t)}{E_k'(z,t)}\right) \quad (10)$$

where $PUR(z,t)$ is the photosynthetically usable radiation and $E_k'(z,t)$ is the spectral photoadaptation parameter [*Arrigo and Sullivan*, 1994]. Both $PUR(z,t)$ and $E_k'(z,t)$ are in units of μEin m^{-2} s^{-1}. Phytoplankton growth is effectively light-saturated when $PUR \approx 3E_k'$. PUR is a function of the spectral irradiance and phytoplankton spectral absorption [*Morel*, 1978]

$$PUR(z,t) = \int_{\lambda=400}^{700} E_d(\lambda,z,t)\frac{a^*(\lambda)}{a^*_{\max}}\,d\lambda \quad (11)$$

where a^*_{max} is the maximum value attained by the phytoplankton absorption coefficient, $a^*(\lambda)$, and $E_d(\lambda,z,t)$ is the spectral downwelling irradiance at depth z and time t. $PUR(z,t)$ is used to calculate PUR^*, a measure of the average amount of usable radiation available during the photoperiod, F, according to the equations

$$\text{if } z \leq \text{MLD}, \ PUR^*(z) = \frac{\int_{z=0}^{MLD} \int_{t=12-F/2}^{12+F/2} PUR(z,t)dt}{F}. \tag{12a}$$

$$\text{if } z > \text{MLD}, \ PUR^*(z) = \frac{\int_{t=12-F/2}^{12+F/2} PUR(z,t)dt}{F}. \tag{12b}$$

In this way, *PUR** represents a value averaged both over the photoperiod and over depth within the mixed layer (i.e., *PUR** will be uniform with depth within the mixed layer), while below the mixed layer, *PUR** represents a value averaged only over the photoperiod (i.e., *PUR** will vary with depth below the mixed layer).

$E_k'(z,t)$ in Eq. 10 varies as a function of *PUR** according to the equations [*Arrigo and Sullivan*, 1994]

$$E_k'(z) = \frac{E_k'_{\max}}{1 + 2\exp[-B \bullet PUR^*(z)]} \tag{13}$$

$$B = \exp\,[1.089 - 2.12 \log (E_k'_{\max})] \tag{14}$$

where $E_k'_{\max}$ is the maximum observed value for E_k'. *Arrigo* et al. [1998a] compiled spectral irradiance data and corresponding values of E_k' for phytoplankton collected over a wide range of times, depths, and locations in the Southern Ocean and determined that $E_k'_{max} \approx 80$ µEin m^{-2} s^{-1}. Equations 13 and 14 scale $E_k'(z)$ with depth to simulate photoacclimation such that $E_k'(z)$ asymptotically approaches $E_k'_{max}$ and $E_k'_{min}$ (=26.4 µEin m^{-2} s^{-1} as defined in Eq. 13) toward the surface and base of the euphotic zone, respectively.

2.2. Defining Regions of Interest

For the purpose of this study, the Southern Ocean (defined as the area south of 50°S) is divided into five geographic sectors (Fig. 1) and four ecological provinces (Fig. 2). Geographic sectors are defined simply by longitude and include the Weddell Sea (60°W to 20°E), south Indian Ocean (20°E to 90°E), southwestern Pacific Ocean (90°E to 160°E), Ross Sea (160°E to 130°W), and Bellingshausen-Amundsen Sea (130°W to 60°W). The four ecological provinces (Fig. 2) are defined based on sea ice coverage and bathymetry and include the pelagic, the MIZ, the continental shelf, and the MIZ-shelf (that part of the MIZ on the continental shelf). Their size is quantified over time by the amount of open water in each (i.e. the size of the shelf province is smaller in the winter than in the summer because it is mostly ice covered during the winter).

Sea ice extent used to define boundaries of ecological provinces is determined from Special Sensor Microwave Imager (SSM/I) data using the PSSM algorithm of *Markus and Burns* [1995]. In this approach, the boundary between sea ice and open water is approximately the 10% sea ice concentration contour. The pelagic province is defined as waters south of 50°S that have been ice-free for >14 days and where water depth is >1000 m. South of the pelagic province is the SIZ which contains the MIZ, the shelf, and the MIZ-shelf provinces. The shelf province is defined as waters with a depth of <1000 m that have been ice-free for >14 days. The MIZ province is associated with the retreating sea ice edge and is defined operationally as any open water pixel where sea ice was present some time in the last 14 days. Anywhere that the MIZ extends onto the shelf is considered part of the MIZ-shelf province. Once a given MIZ or MIZ-shelf pixel has been ice-free longer than the 14 day threshold, it is redefined as being part of the pelagic or shelf province, respectively, depending on water depth. Because of the high temporal variability in the extent of the sea ice cover, the size of all ecological provinces varies daily. The portions of the Patagonian and New Zealand shelves which extend south of 50°S are excluded from all analyses to avoid confusion with productivity on the Antarctic continental shelf.

The threshold for the MIZ of 14 days was calculated from observations of the horizontal distance the surface meltwater layer extended perpendicularly from the ice edge and the number of days taken for sea ice to retreat that distance. Based on three well-documented MIZs, we calculate that low salinity surface waters persist for approximately 14 days after the sea ice has retreated from a given region. After that time, advection and mixing by winds have weakened surface stratification and the phytoplankton bloom collapses. For example, satellite imagery of sea ice extent shows that the ice edge in the Weddell Sea where *Smith and Nelson* [1986] conducted their study was retreating at a rate of 8.3 km d^{-1} (250 km of ice retreat in 30 days). Given that the far edge of the phytoplankton bloom was located 170 km from the ice edge, this suggests that the MIZ persisted for 20 days (170 km/8.3 km d^{-1}=20 days). *Lancelot et al*. [1991] transected the ice edge three times during their study in the spring of 1988. Between their November 26-30 and December 20-24 transects, the ice edge had retreated 160 km, or 6.4 km d^{-1}. The far side of the phytoplankton bloom was 100 km from the ice edge, implying a MIZ persistence time of 15 days. Between the December 20-24 and December 27-31 transect, ice edge retreat had accelerated to a rate of 14 km d^{-1} (100 km in 7 days), resulting in a MIZ persistence time of 10 days (the far side of the phytoplankton bloom was 140 km from the ice edge; 140 km/14 km d^{-1}=10 days). Based on these three values (20, 15, and 10 days, we chose the value of two weeks as a reasonable length of time a pixel should be considered as part of the MIZ.

The primary productivity algorithm is forced with daily input, with the exception of SeaWiFS Chl *a* and OISST, which are 8-eight day means to reduce data gaps due to cloud cover. All model input fields are mapped to a common grid and each pixel is assigned to the appropriate geographic sector (e.g. Weddell Sea, Ross Sea, etc.) and ecological province (e.g. pelagic, MIZ, shelf).

3. Algorithm Validation

3.1. Chlorophyll *a*

The primary productivity algorithm presented here was validated in two steps and consisted of the evaluation of SeaWiFS Chl *a* retrievals using the OC4v4 algorithm [*O'Reilly et al*., 1998] and comparisons of Chl *a*-based primary production obtained *in situ* with those computed by our primary productivity algorithm. Previous efforts to validate SeaWiFS Chl *a* in the Southern Ocean have met with decidedly mixed results. *Barbini et al*. [2006] reported that in the southwestern Ross Sea, the SeaWiFS OC4v4 algorithm overestimated Chl *a* at high concentrations and underestimated them at low concentrations. This is the reverse of what is found in the CCAMLR region of the WAP [*Holm-Hansen et al*., 2004], where SeaWiFS slightly overestimated Chl *a* at concentrations below 0.2 mg Chl *a* m^{-3} and underestimated *in situ* values at higher Chl *a* concentrations. *Garcia et al*. [2005] reported similar underestimates by the OC4v4 algorithm, particularly at concentrations above 0.2 mg Chl *a* m^{-3} for the nearby Bransfield Strait region, with an overall Southern Ocean bias of –21.7%. *Korb et al*. [2004] calculated that in waters around South Georgia Island in the Scotia Sea, SeaWiFS underestimated Chl *a* by only 15% at concentrations below 1 mg Chl *a* m^{-3} but this underestimate increased to 70% at Chl *a* concentrations above 5 mg Chl *a* m^{-3}.

However, a recent analysis by *Marrari et al*. [2006], also for the western Antarctic Peninsula, showed that if *in situ* Chl *a* is determined using high performance liquid chromatography (HPLC), rather than fluorometry, the differences between SeaWiFS-derived Chl *a* and *in situ* Chl *a* virtually disappear. Similarly, *Arrigo and Van Dijken* [2004] used HPLC-derived Chl *a* data from the Ross Sea to show that over a Chl *a* range of 0.2-10 mg m^{-3}, the SeaWiFS OC4v4 algorithm is within 10% of *in situ* values.

Because these validation exercises covered such a limited area of the Southern Ocean, we conducted a larger-scale Chl *a* comparison, similar to that performed earlier by *Sullivan et al*. [1993] for the CZCS. In evaluating SeaWiFS Chl *a* estimates, 5854 *in situ* surface Chl *a* samples were obtained from the NASA SeaBASS bio-optical data archive and compared to Chl *a* estimates derived from SeaWiFS for corresponding regions and time periods. This particular analysis is complicated by three factors, 1) the Southern Ocean *in situ* Chl *a* data set from SeaBASS is heavily biased toward high Chl *a* waters, 2) the data set consists mostly of fluorometrically-derived Chl *a*, and 3) most *in situ* data were obtained before 1997, precluding their direct comparison with SeaWiFS-derived Chl *a*. Nevertheless, we were interested in confirming that the frequency distribution of Chl *a* for the Southern Ocean determined using SeaWiFS is consistent with that generated from *in situ* data.

The bias towards high Chl *a* concentrations in the *in situ* data set is a consequence of the historically high sampling effort in productive regions such as the Ross Sea continental shelf, the Weddell/Scotia Sea, Prydz Bay, and most notably, the WAP, where a single station has been sampled >500 times (Fig. 3). To reduce this high Chl *a* bias as much as possible, we divided the Southern Ocean into five different geographic regions, each of which is analyzed separately. These five regions included the Ross Sea continental shelf, the WAP, the Weddell/Scotia Sea, Prydz Bay, and the "oceanic" Southern Ocean, which consists largely of low Chl *a* waters north of the Antarctic continental shelf.

For all Southern Ocean waters south of 50°S, *in situ* and SeaWiFS estimates of Chl *a* averaged 0.54 and 0.34 mg Chl *a* m^{-3}, respectively (Table 1). Although both data sets exhibited a maximum number of samples in the 0.10-0.15 mg Chl *a* m^{-3} range, there are substantially more *in situ* samples with values above 0.20 mg Chl *a* m^{-3} (Fig. 4a). Many of these high Chl *a* samples were collected in the WAP, which exhibited a relatively large difference between *in situ* and SeaWiFS-derived Chl *a* (Table 1 and Fig. 4b, note the isolated peak at 2.3 mg Chl *a* m^{-3} here and in Fig. 4a). As shown in Fig. 3, most of the *in situ* samples from the WAP were collected in coastal waters while the SeaWiFS analysis included more offshore areas. This disparity resulted in the mean Chl *a* concentration for the *in situ* WAP data (1.91 mg Chl *a* m^{-3}) being almost 4-fold higher than the SeaWiFS-derived estimates for the same region (0.53 mg Chl *a* m^{-3}).

When the high productivity regions of the Southern Ocean are excluded from the analysis, the frequency distributions for Chl *a* determined from *in situ* and from SeaWiFS data are in much better agreement (Fig. 4c), averaging 0.36 mg Chl *a* m^{-3} and 0.28 mg Chl *a* m^{-3}, respectively. As discussed earlier, much of the remaining difference is likely attributable to the fact that the historical *in situ* Chl *a* was determined primarily using fluorometric methods, which overestimate Chl *a* relative to the HPLC method [*Marrari et al*., 2006]. Similarly, frequency plots of *in situ* Chl *a* for the Ross Sea (Fig. 4d), Weddell/Scotia Sea (Fig. 4e), and Prydz Bay (Fig. 4f) are in good agreement with similar plots made from SeaWiFS-derived Chl *a*. These three regions have much more widespread and uniform *in situ* data coverage than the WAP (Fig. 3) and are less heavily biased toward higher coastal values. Although the frequency plots are similar, the mean *in situ* Chl *a* for the Weddell/Scotia Sea (0.92 mg Chl *a* m^{-3}) is about 50% higher than the SeaWiFS-derived value (0.62 mg Chl *a* m^{-3}). This is due to the large number of samples collected near the Scotia Ridge and South Georgia Island (Fig. 3). When these high Chl *a* samples are excluded, the *in situ* mean drops to 0.61 mg Chl *a* m^{-3}, in much better agreement with SeaWiFS data (Table 1).

Consequently. based on our own and previous analyses of SeaWiFS Chl *a* in the Southern Ocean, we conclude that the SeaWiFS OC4v4 algorithm performs adequately when compared to *in situ* Chl *a*, assuming that Chl *a* is determined using HPLC, and when the *in situ* data set is adjusted to account for its bias towards high values. Therefore, we elected to use the standard SeaWiFS OC4v4 Chl *a* values as input to the primary productivity algorithm.

3.2. Primary productivity

Ideally, the primary production algorithm used here would be validated by comparing its output for a specific day and location to measurements made *in situ* at the same time and location. Unfortunately, because of the high degree of phytoplankton patchiness, the large amount of cloud cover in the Southern Ocean, and the relatively few direct field observations collected since 1997, there are too few coincident satellite-derived and *in situ* estimates of production to perform a statistically valid comparison. Instead, we opted to validate our algorithm by first assuming that the SeaWiFS surface Chl *a* retrievals are reliable and then comparing regressions of primary production against surface Chl *a* produced by our algorithm to similar regressions generated using *in situ* Chl *a* and primary production data from the Ross Sea (165°E-165°W, 74°S-78°S) and the Antarctic Peninsula (64°W-73°W, 64°S-68°S). These two locations were chosen because both have ample data from which to derive a statistically significant relationship between Chl *a* and daily primary production and because the dynamic range in both Chl *a* and primary production is large enough to represent the range of variability characteristic of the Southern Ocean.

In the *in situ* primary productivity database for the Antarctic Peninsula, surface Chl *a* ranged from 0.10 to 14.64 mg m^{-3} and primary production from 42.5 to 2466 mg C m^{-2} d^{-1} (n=134). The regression of *in situ* primary production against *in situ* Chl *a* for the Antarctic Peninsula is remarkably similar to a corresponding plot made by regressing SeaWiFS retrievals of Chl *a* against primary production calculated from our primary productivity algorithm for the same geographical region and time period (Fig. 5a). Both exhibit similar shapes and slopes and the range of primary productivity values computed for a given Chl *a* concentration is similar in both data sets. This range in algorithm-derived primary production for a given Chl *a* concentration is due to the fact that regions with similar surface Chl *a* concentration are still likely differ in their solar zenith angle, cloud cover, mixed layer depth, and sea surface temperature and thus will yield different estimates of daily primary productivity.

In the Ross Sea data set, *in situ* Chl *a* ranges from 0.03 to 14.56 mg m^{-3} while the corresponding measurements of primary production range from 156.1 to 2847 mg C m^{-2} d^{-1} (n=95). Again, there is a very good correspondence between the *in situ*- and algorithm-derived regressions of daily primary production against surface Chl *a* (Fig. 5b). Whereas the Antarctic Peninsula data set has a high proportion of observations at Chl *a* concentrations below 2 mg m^{-3}, the Ross Sea has substantially more observations at higher levels of phytoplankton biomass, making it a more appropriate test for high productivity regions of the Southern Ocean. These results suggest that, to the extent that Chl *a* retrievals from SeaWiFS are accurate, the primary productivity algorithm used here produces results that are fully consistent with *in situ* observations of primary production.

4. Results

4.1. Open Water Area

4.1.1. All Southern Ocean Waters

The extent of open water area in the Southern Ocean over an annual cycle varies slightly from year to year between 1997 and 2006, averaging $34.14 \pm 0.23 \times 10^6$ km^2 (Table 2). Open water area exhibits a distinct seasonal cycle (Fig. 6c), increasing rapidly in size from its early spring minimum (27.5×10^6 km^2) to its peak in early March (42.5×10^6 km^2). There is no significant temporal trend with time between 1997 and 2006 in the amount of annual mean open water area in the Southern Ocean (Table 3).

4.1.2. Pelagic province

The pelagic province is by far the largest of the four open-water ecological provinces in the Southern Ocean, averaging $32.0 \pm 0.19 \times 10^6$ km^2 over an annual cycle (Fig. 6b) and accounting for an average of 94% of total open water area south of 50°S (Table 2). When considered over the entire Southern Ocean, the pelagic province exhibits the smallest amount of interannual variability of the four ecological provinces (Fig. 6b), with the coefficient of variation (CV = 100 • standard deviation/mean) of only 0.6% (Table 2). Surprisingly, the proportion of total Southern Ocean area covered by the pelagic province is largest in the winter, despite a much higher sea ice cover in the Southern Ocean during that season. This is because open water in the pelagic province covers a relatively large area of at least ~25×10^6 km^2 in late winter/early spring (Fig. 6b) while the other ecological provinces remain either small (due to a trivial amount of sea ice retreat in the MIZ and MIZ-shelf) or largely ice-covered (e.g., shelf) during the winter. Seasonal changes in open water area are accompanied by a relatively small amount of high-frequency variability compared to the other provinces, particularly the MIZ and MIZ-shelf. This is due to the large size of the pelagic province and the fact that sea ice cover accounts for a much smaller fraction of total area in this province than it does in any of the other three provinces.

4.1.3. MIZ province

The MIZ is the second largest ecological province, covering an annual average of 1.51±0.07 × 10^6 km^2 of the Southern Ocean between 1997 and 2006, and attaining a summer (December) maximum extent of 5.19±0.58 × 10^6 km^2 (Table 2). The largest MIZ is found in the Weddell Sea sector, where it averages 0.44±0.03 × 10^6 km^2 throughout the year, twice as large as the MIZ of the Southwest Pacific Ocean (0.22±0.01 × 10^6 km^2) and the Bellingshausen-Amundsen Sea (0.20±0.02 × 10^6 km^2) sectors. When averaged over an annual cycle, the size of the MIZ exhibits relatively little interannual variability, even when individual geographic sectors are considered (Table 2). However, shorter-term variation in the size of the MIZ can be quite large, particularly in the winter and spring (Fig. 6c). In the most extreme case, the size of the MIZ in the Bellingshausen-Amundsen Sea can vary by as much as 0.6 x 10^6 km^2 over weekly time scales; however short-term variability in the Ross Sea, the Southwest Pacific Ocean, and the Weddell Sea sectors is nearly as large.

4.1.4. Shelf province

The ice-free, non-MIZ, continental shelf is the next largest ecological province in the Southern Ocean, averaging 0.39±0.04 × 10^6 km^2 in area over an annual cycle, with a peak summer open water area of 1.28±0.14 × 10^6 km^2 (Fig. 6d, Table 2). This province is largest in the Bellingshausen-Amundsen Sea (annual mean = 0.13±0.03 × 10^6 km^2) and smallest in the South Indian Ocean and Southwest Pacific Ocean sectors, where its mean annual extent is only 0.04±0.01 × 10^6 km^2. Over the entire Southern Ocean, the CV of the mean annual open water area between 1997 and 2006 is ~10%, much larger than that of any other ecological province (Table 2).

4.1.5. MIZ-shelf province

Smallest of the four ecological provinces is the MIZ-shelf, averaging just $0.25 \pm 0.01 \times 10^6$ km^2 over an annual cycle between 1997 and 2006, with a peak summertime area over the entire Southern Ocean averaging only 0.64×10^6 km^2 (Fig. 6e, Table 2). On average, the MIZ-shelf accounts for approximately 40% of total continental shelf area in the Southern Ocean. Like the MIZ, the size of the MIZ-shelf exhibits marked short-term variability. In addition, the amount of open water area associated with the MIZ-shelf exhibits a great deal of interannual variability with respect to both its magnitude and timing. Maximum open water area associated with the MIZ-shelf is the most variable in the Southwest Pacific Ocean sector, ranging from as low as 0.10×10^6 km^2 in 2000-01 and 2004-05 to as high as 0.18×10^6 km^2 in 1999-00 and 2001-02. Maximum open water area in this sector is usually reached in December or January, in contrast to the Bellingshausen-Amundsen Sea sector, where maximum open water area is not attained until February. In the Ross Sea and the Weddell Sea sectors, the size of the MIZ-shelf usually peaks in December, but may be delayed until as late as February (e.g., 2002-03). In the South Indian Ocean sector in 2004-05 and 2005-06, open water area in the MIZ-shelf did not reach its annual maximum until well into March.

4.2. Primary productivity

4.2.1. All Southern Ocean Waters

Like open water area, daily primary production in the Southern Ocean exhibits a distinct seasonal cycle, increasing exponentially from an average low of ~60 mg C m^{-2} d^{-1} in August to an annual peak in December ranging from 325 to 425 mg C m^{-2} d^{-1}, depending on the year (Fig. 6f). Thereafter, daily primary production exhibits a consistent and rapid decline between January and March, dropping by 75% by the end of the austral summer. Over an annual cycle, daily primary production across the Southern Ocean averages 156 mg C m^{-2} d^{-1} (Table 4), or 57.0 g C m^{-2} yr^{-1}, (Table 4) between 1997 and 2006. The annual peak in primary production precedes the peak in open water area by 2-3 months. Given that the seasonal decline in primary production begins in early summer, prior to refreezing of the ice pack or the autumn increase in wind speeds (and associated vertical mixing and decreased irradiance), the dramatic drop in productivity is most likely attributable to inadequate nutrient supplies, most likely iron [*Arrigo et al*., 2000; *Gervais et al*., 2002; *Coale et al*., 2004], although an increase in grazer populations cannot be discounted. Not surprisingly, interannual variability in primary production is greatest during the spring and summer, when daily rates of production are highest (Fig. 6f).

Total annual primary production in Southern Ocean waters south of 50°S averaged 1949±70.1 Tg C yr^{-1} during the nine years of our study (Table 5). Interannual variability in total production is relatively small, with all years falling within 6% of the mean for the 1997-2006 time period. Productivity is greatest during 1999-00 (2051 Tg C yr^{-1}) and lowest the following year, in 2000-01 (1830 Tg C yr^{-1}), a difference of only 12%. In part, this small degree of interannual variability likely reflects the fact that both the annual mean (33.9 - 34.6 × 10^6 km^2) and maximum (41.9 - 43.1 × 10^6 km^2) open water area in the Southern Ocean vary by <2% between 1997 and 2006 (Table 2).

4.2.2. Pelagic Province

Not surprisingly, the relatively low productivity of the Southern Ocean reflects the dominance of the large pelagic province, where over an annual cycle, daily productivity averages only 148 mg C m^{-2} d^{-1} (Table 4) ranging seasonally from 50-70 mg C m^{-2} d^{-1} in the austral winter to 300-400 mg C m^{-2} d^{-1} at the peak of the spring bloom (Fig. 6g). Annual production in the pelagic province is greatest in the Ross Sea sector of the Southern Ocean (Table 5), averaging 428±29.8 Tg C yr^{-1} between 1997 and 2006, followed closely by the Weddell Sea (412±42.2 Tg C yr^{-1}) and the Bellingshausen-Amundsen Sea (357±14.5 Tg C yr^{-1}) sectors.

Approximately 90% of total annual primary production in the Southern Ocean between 1997 and 2006 is associated with the pelagic province (annual mean = 1729±60.7 Tg C yr^{-1}), due principally to its large size relative to the other ecological provinces, but also to its longer ice-free phytoplankton growing season. This proportion is attributable to the pelagic province is somewhat less than might be expected, however, given that it accounts for an average of 94% of the open water area south of 50°S (Table 2). The reason for this disparity is that the amount of production per unit area (area-normalized production) is lower in the pelagic province than in any of the other ecological provinces (Table 4). Much of the pelagic province remains ice-free year round and thus includes winter months when both the incident irradiance and rates of production are relatively low. In contrast, ecological provinces such as the shelf and MIZ-shelf are ice-free only during the relatively productive spring and summer months, and consequently, have much higher mean daily rates of production (ice-covered regions are not included in calculations of either mean or time-integrated primary production). Like the Southern Ocean as a whole, the pelagic province exhibits relatively little interannual variability in primary productivity, with annual production exhibiting a CV of only 3.5% (Table 5).

4.2.3. MIZ Province

The second largest ecological province, the MIZ is also the second largest contributor to annual primary production in the Southern Ocean, averaging 86.7±12.6 Tg C yr^{-1}. However, because of its relatively small size throughout much of the year, the MIZ accounts for only an average of 4.5% of total primary production in the Southern Ocean (Table 5). Productivity is much more temporally variable in the MIZ than in the pelagic province. Averaged over the Southern Ocean, peak production in the MIZ during the spring phytoplankton bloom ranges from 300 mg C m^{-2} d^{-1} in 2003-04 to >550 mg C m^{-2} d^{-1} in 2004-05 (Fig 6h). In general, daily productivity peaks about a month later (January-February) in the MIZ than in the pelagic province. As expected, peak productivity in the MIZ lags the maximum open water area in this province by 1-2 months (Figs. 6c and 6h), reflecting the time it takes for phytoplankton blooms to fully respond to the newly created ice-free waters associated with the MIZ.

The Weddell Sea sector contains the largest and most productive MIZ in the Southern Ocean, averaging 32.6±5.37 Tg C yr^{-1} (Table 5). This value is 25% greater than in the Ross Sea sector (24.3±3.98 Tg C yr^{-1}) and is at least 300% higher than in the other three geographic sectors.

Interannual variability in total annual primary production within the MIZ is greatest in the Southwest Pacific Ocean sector, varying from 5.99 Tg C yr^{-1} in 2000-01 to 14.4 Tg C yr^{-1} in 1999-00 (Table 5).

Mean area-normalized production in the MIZ is somewhat higher than in the pelagic province, averaging 158 mg C m^{-2} d^{-1} (Table 4), or 57.5 g C m^{-2} yr^{-1} (Table 4). However, given that the MIZ has historically been considered to be a region of enhanced phytoplankton productivity, the small difference in the mean daily rate of primary production between the pelagic province and the MIZ is somewhat surprising. It should be noted that while the mean rate of production over an annual cycle in the MIZ is not much greater than in the pelagic province, the peak daily productivity values in most of the geographic sectors can be twice as high in the MIZ. For example, in the Bellingshausen-Amundsen Sea sector, mean daily production in the MIZ can exceed 1600 mg C m^{-2} d^{-1}, a rate 3-fold higher than the corresponding peak in the pelagic province. In the other geographic sectors, a 2-fold greater peak production in the MIZ than in the pelagic province is not uncommon. These data suggest that while the MIZ can be a very productive marine ecosystem, this is not always the case.

4.2.4. Shelf Province

Considering its small size (Fig. 6d), the continental shelf (non-MIZ) is responsible for a disproportionately high fraction of primary production in the Southern Ocean, contributing 66.1±12.2 Tg C yr^{-1} to the annual total (Table 5). This value is equivalent to 76% of the production of the MIZ despite the shelf being only approximately one quarter the size of the MIZ. In total, the shelf province accounts for approximately 3.5% of total phytoplankton primary production in the Southern Ocean. Mean daily primary production on the continental shelf averages 460 mg C m^{-2} d^{-1}, approximately 3-fold greater than rates in either the MIZ or the pelagic provinces (Table 4). Similarly, mean annual production on the shelf is also relatively high (109 g C m^{-2} yr^{-1}), equivalent to about twice that of the pelagic province.

Productivity on the continental shelf exhibits an annual cycle unlike that of either the pelagic or the MIZ provinces. Daily rates of primary production on the shelf increase linearly and relatively slowly between August and early December throughout the Southern Ocean (Fig. 6i), reaching approximately 200 g C m^{-2} d^{-1} by early December. After that time, primary productivity increases dramatically, with rates increasing 5-10-fold during the month of December. This rapid rise is the result of coincident increases in phytoplankton biomass, downwelling irradiance, and surface ocean stratification during late austral spring. Of particular importance to these high rates of production are the elevated nutrients associated with the Antarctic continental shelves that allow for the accumulation of unusually high concentrations of phytoplankton biomass.

Interannual variability of primary production on the shelf is higher than that of any other ecological province. With total annual production on the Southern Ocean continental shelf ranging from 41.9 Tg C yr^{-1} in 2002-03 to 83.1 Tg C yr^{-1} in 2001-02 (Table 5), the CV is 20% (the CV is only 3.5% for the pelagic province). Peak spring/summer production on the shelf averaged over the Southern Ocean varies from approximately 900 mg C m^{-2} d^{-1} in 2000-01 to 1600 mg C m^{-2} d^{-1} in 2004-05 (Fig. 6i), with the timing of the peak varying from December to February in some sectors. Interannual variation is most extreme in the Ross Sea sector, where maximum production during the spring-summer bloom ranges from a low of 500 mg C m^{-2} d^{-1} in 2002-03 to >2000 mg C m^{-2} d^{-1} in 1998-99 and 1999-00 and total annual production varies >10-fold, from 2.97 Tg C yr^{-1} in 2002-03 to 33.5 Tg C yr^{-1} in 1999-00 (Table 5).

Although the Ross Sea is the most interannually variable, it is also the most productive continental shelf (23.4±9.98 Tg C yr^{-1}), accounting for more than one third of total shelf production in the Southern Ocean (Table 5), despite comprising only 20% of ice-free shelf area (Table 2). Next in importance are the Bellingshausen-Amundsen Sea (14.9 Tg C yr^{-1}) and the Weddell Sea (13.7 Tg C yr^{-1}) sectors, each of which account for a little more than 20% of total shelf production in the Southern Ocean. Although the South Indian Ocean and Southwest Pacific Ocean sectors contain similar amounts of ice-free shelf area (0.37-0.38 $\times 10^6$ km^2, Table

2), the shelf of the former sector is approximately twice as productive as that of the latter (Table 6), due to its much higher area-normalized rate of production (Tables 4 and 5). Together, these two sectors account for a little less than 20% of total shelf production in the Southern Ocean

4.2.5. MIZ-shelf Province

Due in part to its minor amount of open water area, the MIZ-shelf is the smallest contributor to annual production of the four ecological provinces, adding an average of 27.3±4.67 Tg C yr^{-1} (1.4%) to total phytoplankton production in the Southern Ocean. The MIZ-shelf exhibits enhanced mean daily rates of production relative to both the MIZ and pelagic provinces, averaging 303 mg C m^{-2} d^{-1}, but interestingly, this value is only about 66% of the average rate on the non-MIZ continental shelf. Thus, the productivity of the MIZ-shelf is intermediate between the MIZ province and the shelf province, at least in terms of both mean daily and mean annual area-normalized production (Table 4).

Lending support for the notion that the MIZ-shelf behaves more like the shelf province than like the MIZ is the fact that its annual cycle of daily production (Fig. 6j) closely resembles that of the shelf province (Fig. 6i), increasing slowly between August and early December, then rising rapidly before peaking in late December or January. This pattern is clearly discernable in all geographic sectors, with the possible exception of the Ross Sea, where the typical pattern is not as obvious due to unusually early and rapid increases in productivity during some years. Peak production in the MIZ-shelf is nearly as high as in the shelf province, with mean daily production exceeding 1000 mg C m^{-2} d^{-1} throughout most of the Southern Ocean, and occasionally exceeding 1500 mg C m^{-2} d^{-1}.

Interannual variability is also high in this ecological province, almost as high as that of the continental shelf (Table 5). Much of this variability is associated with the rapid rise in production observed after early December. This time period is characterized by rapid changes in open water area (Fig. 6e), and consequently, daily-weekly changes in production can be large and highly variable between years (Fig. 6j). Peak production during the spring/summer bloom ranges from <800 mg C m^{-2} d^{-1} in 2004-05 to >1300 mg C m^{-2} d^{-1} in 2001-02. In the Ross Sea sector, peak spring/summer production is particularly variable, ranging from <400 mg C m^{-2} d^{-1} in 2002-03 to ~2000 mg C m^{-2} d^{-1} in 2001-02. Like the shelf province, timing of the peak of the bloom on the MIZ-shelf also varies markedly between years, ranging from early December to mid-February in both the Weddell Sea and Ross Sea sectors.

As with the shelf province, production on the MIZ-shelf is greatest in the Ross Sea sector (7.84±2.24 Tg C yr^{-1}), although the inter-sector differences in this ecological province are not nearly as large as on the shelf (Table 5). With a rate of 7.17±1.38 Tg C yr^{-1}, the MIZ-shelf of the Bellingshausen-Amundsen Sea sector is similar to that of the Ross Sea sector, although the amount of open water area on the MIZ-shelf is much lower in the Ross Sea sector (Table 2). The Ross Sea sector compensates for its relatively smaller ice-free MIZ-shelf by having the highest area-normalized rates of production (485 mg C m^{-2} d^{-1} and 81.9 g C m^{-2} yr^{-1}) of any of the geographic sectors (Tables 4 and 5). Together, the Ross Sea and Bellingshausen-Amundsen Sea sectors account for 55% of the total annual production in the Southern Ocean MIZ-shelf. The Weddell Sea sector accounts for 22% of total MIZ-shelf production, while the Southwest Pacific Ocean and the South Indian Ocean sectors account for 11% and 10%, respectively.

4.3. Spatial patterns in primary production

To determine the physical factors most responsible for spatial and temporal patterns in annual primary production in the Southern Ocean, we calculated mean annual primary production (Fig. 7a) and regressed annual production anomalies (Fig. 8) against anomalies of mean annual Chl *a* concentration (Fig. 9), mean annual sea ice coverage (Fig. 10), and mean annual sea surface temperature (Fig. 11). Not surprisingly, annual production anomalies are highly positively correlated with Chl *a* anomalies throughout the Southern Ocean (Fig. 12a), with annual variations in Chl *a* explaining from ~50% to almost 100% of the interannual variability in mean annual production between 1997 and 2006. This high correlation is a consequence of the fact that primary productivity is calculated as the product of surface Chl *a* and the estimated phytoplankton growth rate (Eq. 7). Because Chl *a* can vary by four orders of magnitude in the Southern Ocean, much more so than does the phytoplankton growth rate in open water when the sun is above the horizon, variations in production are largely driven by changes in surface Chl *a*. Of course, at a given Chl *a* concentration, phytoplankton growth rate will still vary considerably depending on spatial and temporal differences in ambient irradiance and water temperature. This environmental variability explains why there is a sizable range in daily production computed by the primary production algorithm for a given Chl *a* concentration, as shown in Fig. 5.

Within the SIZ of the Southern Ocean, annual production anomalies (Fig. 8) are also related to anomalies in sea ice distributions (Fig. 10), with some locations exhibiting a positive correlation and others a negative one (Fig. 12b). Negative correlations are strongest near the coast where temperatures are lowest and sea ice persists for a longer period of time (Figs. 7c and 7d). In these regions, the presence of annual sea ice typically restricts the length of the phytoplankton growth season and thus limits annual production. Consequently, the coastal zone is particularly sensitive to changes in sea ice dynamics. This pattern is clearly evident in the Southwestern Pacific Ocean sector where years with an anomalously short sea ice season, such as in 2001-02 (Fig. 10), also exhibit anomalously high annual primary production in the coastal zone (Fig. 8).

Farther offshore, the relationship between sea ice anomalies and annual primary production anomalies becomes more complex. There are obvious instances where an anomalously long sea ice season (Fig. 10) leads to the expected low annual production anomaly (Fig. 8), such as in both the WAP and Scotia Sea in 1997-98. Conversely, some areas where the sea ice season is anomalously short have anomalously high annual production. Good examples include the western Weddell Sea sector in 1999-00 and 2001-02 and the Ross Sea sector in 2001-02 and 2005-06. In other regions, however, sea ice anomalies are positively correlated with annual production anomalies. This counterintuitive result stems from annual production being either higher during years when sea ice persists for a longer period of time or lower when sea ice retreats earlier in the year. This pattern is particularly evident in the western Weddell Sea sector in 1999-00 and 2005-06 (compare Figs. 8 and 10) but is also seen in the eastern Ross Sea sector at approximately 70°S in 2001-02. Closer inspection reveals that positive correlations between annual production anomalies and sea ice anomalies (Fig. 12b) are restricted predominantly to waters where production in the MIZ province is important, such as in the Weddell Sea and offshore waters of the Ross Seas (blue areas in Fig. 12d). In these waters, anomalously low sea ice will reduce both the size of the MIZ and possibly the degree of surface water stratification within any MIZ that does develop. Because the MIZ can be more productive than the pelagic province, a loss of MIZ area will reduce annual primary production. Thus, there is generally a high correspondence between regions that exhibit a high positive correlation between annual primary production and sea ice anomalies (red areas in Fig. 12b) and the approximate position of the MIZ, as can be seen clearly for the spring bloom of 1998-99 (blue areas in Fig. 12d).

A map of the correlation between annual primary production anomalies (Fig. 8) and annual SST anomalies (Fig. 11) suggests that a complex relationship also exists between these two quantities (Fig. 12c). This is likely due to the fact that SST can impact rates of production directly, through the relationship between temperature and phytoplankton metabolic rate (Fig 4), and indirectly, via its impact on surface ocean stratification and sea ice distributions. In general, waters north of the SIZ tend to exhibit a positive correlation between SST anomalies and annual production anomalies, with the highest correlation coefficients found in the Ross Sea, Bellingshausen-Amundsen Sea, and South Indian Ocean sectors (Fig. 12c). SST anomalies in these regions frequently exceed ±1.2°C, although anomalies of ±0.4°C are more typical. The positive correlation between anomalies of SST and annual production in these ice-free waters is the result of increased phytoplankton growth rates at higher temperature. High positive correlations are also apparent within the SIZ of the Weddell Sea, the Ross Sea, and the Amundsen Sea sectors and in nearshore waters of the South Indian Ocean sector. In these regions, positive SST anomalies are frequently associated with negative sea ice anomalies (e.g., the western Weddell Sea in 1998-99, the nearshore South Indian Ocean in 1997-98, the eastern

Ross Sea in 2003-04, Figs. 10 and 11). In these cases, the high positive correlation between anomalies of SST and annual production are the result of reduced ice cover and increased light availability. Whether the ice cover is reduced because of the anomalously SST or SST is high due to reduced ice cover is not apparent.

Regions exhibiting a strong negative correlation between anomalies of SST and mean annual production are predominantly restricted to the SIZ of the South Indian Ocean and a large fraction of the Southwestern Pacific Ocean sector (Fig. 12c). In these waters, positive SST anomalies (Fig. 11) are associated with negative mean annual production anomalies (Fig. 8). There is no clear relationship between SST anomalies and sea ice anomalies in these waters, suggesting that the negative correlation between anomalies of SST and mean annual production are the result of reduced nutrient supply in waters stratified by higher temperatures, rather than by increased sea ice melt.

4.4. Temporal Trends in annual production

4.4.1. Secular trends

Over the nine-year time frame of this study, there is no significant temporal increase or decrease in total annual production within the Southern Ocean, with advancing year explaining only 11% of the interannual variability (Table 3). However, the passage of time has more explanatory power when the Southern Ocean is divided into geographic sectors. Both the Ross Sea and the South Indian Ocean sectors exhibit statistically significant changes in annual production between 1997 and 2006 (Table 3), with production in the Ross Sea increasing by nearly 9 Tg C yr^{-1} yr^{-1} ($R^2 = 0.54$, p=0.024) and production in the South Indian Ocean dropping by >4 Tg C yr^{-1} yr^{-1} ($R^2 = 0.46$, p=0.046). Changes in annual production over time in both the Ross Sea and the South Indian Ocean sectors are most pronounced (and statistically significant) in the pelagic province (Fig. 13a). The relationship between primary production and year is stronger in deep water, offshore environments than it is in the nearshore or coastal environments of the Southern Ocean (Fig. 13a).

In general, interannual variability in annual production is more closely tied to changes in open water area than to the passing of time. For the entire Southern Ocean, there appears at first glance to be no relationship between annual primary production and mean annual open water area (R^2=0.004, Table 3). However, within the Southern Ocean there is a statistically significant relationship between annual primary production and open water area in all of the ecological provinces except for the pelagic, with the relationship between these two quantities being particularly strong in nearshore environments (Fig. 13b), such as on the continental shelf (R^2=0.76, p=0.002). Furthermore, every geographic sector contains at least one ecological province, and four out of the five contain two ecological provinces (South Indian Ocean is the lone exception), that exhibit a statistically significant relationship between annual primary production and open water area (Table 3). In all of these cases, as open water area increases, so does annual production, at a rate of approximately 100-300 Tg C for every additional million km^2 of open water area. For example, the shelf province exhibits a statistically significant relationship between annual production and open water area in four out of five geographic sectors, while the pelagic province varies significantly with open water area in only a single geographic sector (the Ross Sea). Thus, it appears that the poor relationship between annual primary production and advancing year is a consequence of the fact that open water area also exhibits little evidence of a secular trend through time (Fig. 13c). Only the pelagic province of the Ross Sea exhibits a statistically significant change (R^2=0.46, p=0.045) in open water area through time (Table 3).

4.4.2. The Southern Annular Mode

The Southern Annular Mode (SAM) is the dominant climate pattern of the Southern Ocean and is characterized by the north-south atmospheric pressure gradient and thus, the strength of the westerly winds, with the positive phase of the SAM exhibiting stronger than normal winds. Strong westerly wind anomalies associated with a positive SAM have been proposed to intensify divergence near the Antarctic Polar Front zone and result in increased upwelling of cooler, deep waters rich in nutrients, thus fueling the production of phytoplankton biomass [*Lovenduski and Gruber*, 2005]. This proposed pattern is consistent with our results showing that a significant relationship exists between the SAM and interannual changes in mean annual SST in the Southern Ocean (R^2=0.52, p=0.029), with SST being lower during the high upwelling events associated with a positive SAM (Table 6). The impact of the SAM on SST seems to be particularly strong in the Ross Sea sector (slope= -0.371, p=0.004) and the adjacent Southwest Pacific Ocean sector (slope= -0.400, p=0.015) and much weaker in the South Indian Ocean and Weddell Sea sectors. Not surprisingly, this trend in Southern Ocean SST with SAM is most pronounced in the pelagic province (R^2=0.47, p=0.041), which is the ecological province in closest proximity to the Antarctic divergence zone.

Despite its correspondence with SST, the SAM explains a much smaller amount of the interannual variability in mean surface Chl *a* in the Southern Ocean (Table 6). Only the shelf province of the Ross Sea exhibited a strong and statistically significant relationship (slope = 0.826, p=0.009) between interannual changes in Chl *a* and the SAM (Table 6). Similarly, there was no statistically significant relationship between total annual primary production in the Southern Ocean and the annual mean SAM index (R^2=0.31, p=0.123). Although interannual trends in annual production closely track year-to-year changes in the SAM index between 1999 and 2006 (Fig. 14), there were too few data points (only 9 years) for the relationship to be significant.

5. Discussion

5.1. Comparison with Previous Primary Production Estimates

Annual primary production estimates reported here for all Southern Ocean waters south of 50°S are lower than previous satellite-based calculations made for this region. Using Chl *a* data from SeaWiFS and the VPGM algorithm of *Behrenfeld and Falkowski* [1997], *Moore and Abbott* [2000] estimated total production south of 50°S to be 2850 Tg C yr^{-1}, 46% higher than our average for 1997-2006 of 1949 Tg C yr^{-1}. Considering that the VPGM algorithm was developed for use with global data and was not parameterized specifically for use in the Southern Ocean, this difference is not surprising. However, using monthly ocean color data from the CZCS and a productivity algorithm very similar to that used here, *Arrigo et al*. [1998a] estimated that annual production in the Southern Ocean varies from 3241 to 4414 Tg C yr^{-1}, values that are 66-126% higher than our estimate. The higher estimates of production obtained by Arr*igo et al.* [1998a] are attributable to the higher Chl *a* concentrations produced by the CZCS for the Southern Ocean. Retrievals of Chl *a* by the CZCS were notoriously difficult in the Southern Ocean, a region where long atmospheric path lengths coupled with phytoplankton having unique bio-optical properties resulted in satellite-based Chl *a* estimates that were much less robust than those obtained for other ocean basins [*Sullivan et al*., 1993]. In addition, the CZCS algorithm generated estimates of pigment concentration, rather than Chl *a*. Although attempts were made by *Arrigo et al*. [1998a] to reconcile these two variables, there has been no reliable way to convert Southern Ocean surface pigment concentration to Chl *a* over large spatial scales due to a lack of *in situ* pigment data. Correction factors were applied to the CZCS data to force them to conform to observations [*Sullivan et al*., 1993], but the efficacy of these corrections was difficult to evaluate, and likely resulted in overestimates of Chl *a*, particularly in mesotrophic offshore waters [*Moore and Abbott*, 2000]. Therefore, although they are significantly lower, because the estimates of annual primary production presented here are based on the more reliable Chl *a* retrievals from SeaWiFS, they are likely to be more accurate than those presented in *Arrigo et al*. [1998a].

Furthermore, a comparison of global output from 24 satellite-based primary production algorithms (including ours) shows that agreement between algorithms is especially poor for the Southern Ocean, with annual production ranging from 1100 to 4900 Tg C yr^{-1} and averaging 2600 Tg C yr^{-1} [*Carr et al*., 2006]. The large divergence between algorithms was attributed primarily to the differences in the way they formulated primary production as a function of temperature. In some algorithms, production was assumed to vary independent of temperature, while in others temperature exerted a strong influence on productivity. As a result, the extremely low temperatures characteristic of many Southern Ocean waters (<0°C) resulted in estimates of primary production by the 24 algorithms that varied over a range of 372% [Table 3 in *Carr et al*., 2006]. Although the analysis by *Carr et al*. [2006] did not include an assessment of which of the 24 satellite-based estimates agreed best with *in situ* measurements of primary production, they noted that only two of the 24 algorithms were parameterized specifically for the Southern Ocean (ours was one) and only three of the 24 included any Southern Ocean data during model parameterization. Hence, the use of algorithms not parameterized for the Southern Ocean is likely to result in estimates of primary production that differ significantly from those presented here.

Because of the increased abundance of high quality HPLC-derived pigment data from the Southern Ocean, and the larger number of *in situ* estimates of daily primary production used to parameterize our algorithm, we believe that the lowered estimates of annual production in the Southern Ocean reported here are probably more realistic than past large-scale estimates. Based on a relatively large number of Southern Ocean analyses of SeaWiFS data [*Arrigo and Van Dijken*, 2004, *Korb et al*., 2004; *Garcia et al*., 2005; *Marrari et al*. 2006], it is unlikely that surface Chl *a* in the Southern Ocean is being underestimated by more than 20%, and probably much less than that, particularly in the open ocean where pigment concentrations are relatively low and account for the bulk of production. Furthermore, rates of primary production for a given concentration of Chl *a* calculated by our algorithm agree very well with a wide range of observations made in the Southern Ocean (Fig. 5). If true, the Southern Ocean is considerably less productive than has been assumed over much of the past decade, with annual production rates equivalent to approximately 41-70% of previous estimates [*Longhurst et al*., 1995, *Arrigo et al*., 1998a; *Moore and Abbott*, 2000; *Reuer et al*., 2007]. Rather than representing approximately 10% of global marine primary production [*Arrigo et al*., 1998a], our results suggest that the Southern Ocean accounts for less than 5% of this amount.

5.2. The Productive MIZ?

Given that the MIZ historically has been considered to be a region of enhanced primary productivity, the small differences in both daily and annual area-normalized rates of production between the generally low productivity pelagic province and the MIZ province are somewhat surprising. Although some of this similarity may be attributable to the operational definition of a MIZ used in the present study, this is not likely to be the primary reason. We defined the MIZ province as consisting of those pixels that have been ice-free for no longer than 14 consecutive days. Once this threshold has been reached, the pixel is redefined as either a pelagic or MIZ-shelf pixel, depending upon water depth. If our 14 day threshold is much shorter than the lifetime of a typical MIZ, any productivity that should be attributed to the MIZ will have been associated with the pelagic or MIZ-shelf province. The seriousness of this underestimate of MIZ production will depend on how long it takes for phytoplankton to bloom after the sea ice retreats. If the MIZ phytoplankton bloom takes longer than 14 days to reach its peak, production in the MIZ will be underestimated using a 14 day threshold. *Lancelot et al*. [1991] noted that in the Weddell-Scotia Sea, the region of maximum water column Chl *a* in the MIZ was consistently located within 0.5° (56 km) of the ice edge during the spring of 1988. Given a rate of sea ice retreat of 6-14 km d^{-1} (see section 2.2), peak Chl *a* concentrations must have been reached 4-9 days after sea ice retreat, well within our 14 day threshold. This conclusion is supported by the large number of high productivity events associated with the MIZ during spring and summer in our study (Fig. 6h), suggesting that phytoplankton are attaining high levels of biomass and rates of production within the 14 day threshold used to define the MIZ.

In two previous studies of primary production in the Southern Ocean, the MIZ was defined as the region of open water in a given month that had been ice-covered the previous month [*Arrigo et al*., 1998a; *Moore and Abbott*, 2000]. Both of these studies calculated productivity (and the size of the MIZ) from monthly mean data, including both sea ice and Chl *a* data, and thus the MIZ was assumed to persist for approximately 30 days, twice as long as was assumed in the present study. In the investigation by *Arrigo et al.* [1998a], the MIZ accounted for 9.5% of total primary production in the Southern Ocean, much higher than the 4.4% estimated for the MIZ in the present study. It is unlikely however, that this difference can be attributed to the longer-lived MIZ assumed by *Arrigo et al.* [1998a]. This is because *Moore and Abbott* [2000] also used a 30 day threshold for the MIZ and they estimated a mean rate of production within the MIZ of 54.2 g C m^{-2} yr^{-1}, very close to our estimate of 57.5 g C m^{-2} yr^{-1}. Moreover, the MIZ in their study accounted for 3.3% of total annual primary production, much less than the estimate of 9.5% by *Arrigo et al*. [1998a] who used the same 30 day threshold, and even slightly lower than the estimate of 4.4% made here using a 14 day threshold.

These results indicate that the calculated production of the MIZ is more closely tied to the Chl *a* field used as algorithm input than it is to the assumed lifetime of the MIZ. The present study and the study by *Moore and Abbott* [2000] both used SeaWiFS data to specify phytoplankton distributions and obtained similar results for MIZ production (despite using MIZ lifetimes of 14 days and 30 days, respectively) while *Arrigo et al.* [1998a] used CZCS data and obtained much higher estimates of MIZ production (despite using the same MIZ lifetime as that used in the present study). Chl *a* in regions of high sea ice cover were often overestimated by the CZCS due to incomplete masking of sea ice contaminated pixels [*Arrigo and McClain*, 1995]. This problem would have been most serious in the MIZ where sea ice can be present at concentrations low enough to be missed by the sea ice masking algorithm. Largely corrected in the SeaWiFS data, overly high estimates of Chl *a* by the CZCS in the MIZ may explain why estimates of MIZ production by *Arrigo et al*. [1998a] are so much higher than those presented here and by *Moore and Abbott* [2000].

Why then is the MIZ only slightly more productive than the pelagic province? If not an artifact of our analyses, then the lower than expected productivity of much of the MIZ must be attributable to conditions not always being conducive for intense phytoplankton blooms. While it is true that maximum rates of daily primary production are much higher in the MIZ (Fig. 6h) than in the pelagic province (Fig. 6g), it is also true that the minimum values in the MIZ are substantially lower than in the pelagic. This trend applies to all geographic sectors as well as during the peak spring-summer phytoplankton bloom season. For example, while maximum rates of primary production in the MIZ of the Bellingshausen-Amundsen Sea often exceed 600 mg C m^{-2} d^{-1} for short periods of time, more often, rates of production during the peak of the spring bloom (December-January) are in the range of 200-250 mg C m^{-2} d^{-1}. In contrast, although there were not as many high productivity bloom events in the pelagic province of the Bellingshausen-Amundsen Sea, primary production in late December-early January exceeded 300 mg C m^{-2} d^{-1} during each of the nine years of our study. Thus, although the MIZ province experiences more high productivity blooms than the pelagic, it is also characterized by lower non-bloom rates of production.

One explanation for this is that much of the MIZ of the Southern Ocean either never develops a well-stratified upper mixed layer or the mixed layer is destroyed by wind-driven turbulent mixing before a phytoplankton bloom can form [*Fitch and Moore*, 2007]. By definition, the MIZ is an area of open water within the SIZ that has recently been covered with sea ice. While still ice covered, there is little chance of appreciable phytoplankton growth due to low light transmission through the snow, sea ice, and associated particulate material [*Arrigo et al*., 1991], and phytoplankton abundance will be low. Once the sea ice has left an area due to advection and/or melting, phytoplankton can grow, given sufficient light and nutrients, although initial Chl *a* concentrations will be low unless there is an appreciable contribution of algal cells from melting sea ice. In the absence of a well-stratified mixed layer, phytoplankton biomass and rates of primary production in the MIZ will remain low. Similarly, even when a stratified mixed layer does develop, if it does so in offshore waters that are low in micronutrients such as Fe (macronutrients are in ample supply over most of our study region), nutrients will be rapidly exhausted and primary production also will be low. As can be seen from the small fraction of total SIZ area exhibiting a strong positive correlation between primary production and sea ice distributions (Fig. 12b, sea ice and primary production are only positively correlated in the MIZ), conditions favoring phytoplankton blooms in the MIZ are relatively uncommon and account for a small fraction of total MIZ area. Thus, while the MIZ is large and has the potential to be biologically productive, physical conditions there are seldom conducive to the development of intense, longer-lived phytoplankton blooms.

In addition to daily rates of primary production in much of the MIZ that are relatively low due to unfavorable growth conditions, annual rates are also low. This is due in part to the modest daily rates, which are, on average, only 7% higher than in the pelagic province, but also to the shorter growing season characteristic of the MIZ. The impact of growing season can be seen most clearly by comparing distributions of Chl *a* (Fig. 7b) and annual primary production (Fig. 7a). Despite the fact that the SIZ and MIZ have mean Chl *a* concentrations that are higher than in pelagic waters north of the SIZ, annual production in the MIZ and the pelagic province are similar in magnitude (57.5 and 54.0 g C m^{-2} yr^{-1}, respectively). The high Chl *a* concentrations in the SIZ are somewhat misleading because they only reflect values when waters have become ice-free; they do not include concentrations below the sea ice that would undoubtedly reduce the annual mean substantially. Nevertheless, the length of the growing season, which can be inferred from Fig. 7c by subtracting a given pixel value from the number 365 (or 366 for leap years), is substantially shorter in the SIZ and MIZ than it is throughout much of the pelagic; most of the SIZ and MIZ have growing seasons that are less than half as long as those north of the SIZ. Consequently, rates of annual production in the MIZ differ little from corresponding values in the pelagic province. Similarly, a reduced growing season in the MIZ also explains much of why productivity in the MIZ-shelf province is so much lower than in the (non-MIZ) shelf (Tables 4 and 5).

5.3. Interannual Variability in Primary Productivity

Annual primary production in the Southern Ocean exhibited a surprisingly small amount of interannual variability between 1997 and 2006, varying by only ±11% (computed as [maximum-minimum]/mean). This is significantly less interannual variability than has been measured in other ocean basins. For example, annual net primary production varied by 30% or more over large stretches of the tropical Pacific Ocean between 1999 and 2004 [*Behrenfeld et al*., 2006].

Much of this variability is attributable to ENSO-driven changes in upper ocean temperature and stratification, changes that are not manifested nearly so severely in the Southern Ocean. *Lomas and Bates* (2004) documented an extremely high degree of interannual variability in primary production (121%) in the western north Atlantic tropical gyre from 1992 to 2000. This large variability derives primarily from interannual changes in nutrient input via deep convective mixing driven by the passage of storms [*Steinberg et al*., 2001]. Because nutrient inventories in the relatively shallow upper mixed layer of the tropical gyres are so low, phytoplankton growth rates in these waters are particularly sensitive to changes in nutrient input. This sensitivity to nutrient supply is in stark contrast to the Southern Ocean where mixed layers are deep, relative changes in nutrient inventories of the upper ocean are modest, and variability in production is attributable primarily to changes in light environment (via variations in sea ice extent). A good example of this is the WAP where the observed order of magnitude changes in primary production from year-to-year are related to the amount of open water within the annual ice pack [*Ducklow et al*., 2006].

Interannual variability in annual production in the Southern Ocean also is lower than in other polar and sub-polar waters. For instance, interannual variability of primary production in the North Sea is around 15% [*Skogen and Moll*, 2000], slightly higher than the 11% reported here. More significantly, estimates of annual primary production in the Arctic Ocean (all waters north of the Arctic Circle) made over the same nine-year period as the present study varied from 375 to 483 Tg C yr^{-1}, an interannual range of 26% [*Pabi and Arrigo*, submitted]. These interannual differences in Arctic primary production are attributable primarily to the dramatic changes in ice-free area over the past decade, which has increased by ~75,000 km^2 yr^{-1} since 1998. As was observed in the present study of the Southern Ocean, interannual changes in Arctic waters are most dramatic on the continental shelves, which make up a much larger fraction of total area in the Arctic (53%) than they do in the Antarctic.

Although interannual changes in the amount of open water in the Southern Ocean were not significantly correlated with annual rates of primary production (Table 3), a strong relationship exists between the degree of interannual variability in open water area in a given region and interannual variability in annual primary production (interannual variability is quantified as the ratio of the maximum to the minimum mean annual value for each geographic sector and ecological province, Fig. 15). Not surprisingly, regions exhibiting the greatest interannual range in open water area (e.g., the Ross Sea shelf) also exhibited the largest range in annual primary production. What is surprising is that the data from all of the geographic sectors and ecological provinces can be explained by a single relationship $Y = 0.45 \exp(0.9543X)$, $R^2=0.85$, $p<0.001$), despite the fact that each region exhibits a very different relationship between annual primary production and mean annual open water area (Table 3). Two important conclusions can be drawn from this relationship. First, interannual variations in production are driven primarily by changes in sea ice cover, although changes in nutrient delivery (most likely iron) to surface waters induced by processes associated with atmospheric variability (e.g., SAM) also likely play a role. Second, the relationship between min:max open water area and min:max annual production (integrated over the Southern Ocean) is not linear, with annual primary production changing more rapidly than the change in open water area. This reflects the fact that when open water increases, both the total area suitable for phytoplankton growth and the area-normalized rates of production increase.

Open water in the Arctic has increased dramatically since 2002, with an associated increase in annual primary production [*Pabi and Arrigo*, submitted]. Similar secular trends have not been observed in the Antarctic, with the exception of the Bellingshausen-Amundsen Sea, where increasing temperatures between 1957 and 1998 are associated with a substantial loss of sea ice [*Turner et al*., 2007]. Increases in temperature in the Antarctic Peninsula region and a slight cooling within much of the Antarctic interior have been attributed to a shift toward a positive phase of the SAM that began in 1957, the result of decreased stratospheric ozone concentrations. This loss of ozone has generated colder tropospheric temperatures over the Antarctic continent, a larger meridional pressure gradient, and increased westerly winds near 60°S [*Thompson and Solomon*, 2002]. These more intense westerlies are thought to warm the Antarctic Peninsula by decreasing the incidence of cold air outbreaks from the Antarctic interior, leading to increased advection of warmer air from the Southern Ocean [*Thompson and Solomon*, 2002]. However, this proposed scenario is complicated by the fact that the climate of the Antarctic Peninsula also is strongly affected by teleconnections with the tropics [*Turner et al*., 2007]. During El Niño, higher mean sea level pressure over the Bellingshausen Sea results in a cooling of the Antarctic Peninsula. Furthermore, recent El Niño events have been more intense and more frequent, which would be expected to result in cooling trend in the region, rather than the rapid warming that has been measured over the past few decades [*Turner et al*., 2007]. It is clear that the causes of the warming in the Antarctic Peninsula region have not yet been fully elucidated.

The lack of a secular trend in both sea ice extent and phytoplankton productivity likely can be attributed to the lack of a warming trend over much of the Antarctic due to the shift to a positive phase of the SAM over the last half century. This shift has resulted in little or no change in temperature over much of the Antarctic, with the exception of the Antarctic Peninsula, and no long-term trend in sea ice concentration. Because the recent long-term shift to a positive SAM has been tied to reductions is stratospheric ozone resulting from increased CFC production, it is possible that warming and loss of sea ice in the Southern Ocean would have been more extreme in recent decades had the Antarctic ozone hole not developed [*Thompson and Solomon*, 2002].

5.4. Future Changes in Southern Ocean Primary Production

Changes in Southern Ocean circulation and biogeochemistry have proven to be difficult to predict due to a limited observational database and an inability of many large-scale models to accurately represent important physical, chemical, and biological processes. In a comparison of 18 coupled climate models included in the IPCC Fourth Assessment Report, *Russell et al.* [2006a] noted the wide range in model predictions of water mass transformations and the strength and position of the westerly wind belt, key components in the ability to predict anthropogenic CO_2 uptake and changes in biological productivity. One area of general agreement among models is that stratification of the surface Southern Ocean is likely to increase over the next century in response to changes in atmospheric CO_2 and temperature [*Sarmiento et al.*, 1998; *Caldeira and Duffy*, 2000; *LeQuere et al.*, 2007]. This increase in stratification will reduce both the ability of the surface ocean to remove atmospheric CO_2 and the flux of nutrients from the deep ocean, thereby reducing phytoplankton growth and productivity. In a recent model that was better able to simulate the poleward intensification of the westerly winds [*Russell et al.*, 2006b], it was predicted that storage of heat and anthropogenic CO_2 would actually increase in the future due to a larger outcrop area of the dense waters around Antarctica and more intense divergence, thereby counteracting the effect of increased stratification of most of the Southern Ocean.

This predicted increase in divergence could increase the flux of micronutrients into the Polar Front zone and into waters further south, thereby increasing phytoplankton growth and productivity. Although the magnitudes of Chl *a* concentrations and primary production have been shown here to respond weakly, but positively, to increased divergence associated with the SAM (Table 6), these effects might be much larger under conditions of increased divergence in the future. On the other hand, the meridional pressure gradient that has intensified in recent decades due to the stratospheric cooling associated with the Antarctic ozone hole [*Thompson and Solomon*, 2002] may diminish in coming years as stratospheric CFC concentrations drop and the Antarctic ozone hole dissipates. How the balance between these two large global perturbations will impact biogeochemistry in the Southern Ocean has yet to be determined.

Finally, in addition to aforementioned changes in the Southern Ocean predicted for the upcoming century (increased westerly winds, stronger Antarctic divergence, increased surface ocean stratification) is a 17-31% reduction in sea ice extent, assuming a doubling of atmospheric CO_2 by 2100 [Rind *et al.*, 1997; Meehl *et al.*, 2000]. *Arrigo and Thomas* [2004] predicted that a 25% decrease in sea ice would result in a 10% increase in total primary production, with increases in production north of the ice edge outpacing losses in the diminished areas of the MIZ and SIZ. However, their analysis assumed that rates of production in the MIZ were substantially higher than those in the pelagic province. Our results (and similar results in *Moore and Abbott,* 2007), suggest that this is not the case, that average rates of daily primary production in the MIZ are very similar to those in the pelagic province. Thus, the predicted losses of production due to a diminished size of the MIZ will not be as large as those assumed by *Arrigo and Thomas* [2004]. Consequently, the net increase in total production in the Southern Ocean in response to a reduced sea ice cover should be a few percent larger than the 10% predicted by *Arrigo and Thomas* [2004].

References

Arrigo, K. R. and C. W. Sullivan (1994), A high resolution bio-optical model of microalgal growth: Tests using sea ice algal community time series data, *Limnol. Oceanogr.*, *39*, 609-631.

Arrigo, K.R. and C.R. McClain (1995), Cloud and ice detection at high latitudes for processing of CZCS imagery. NASA Technical Memorandum 104566, Vol. 28, SeaWiFS Technical Report Series.

Arrigo, K. R. and D. Thomas (2004), Large scale importance of sea ice biology in the Southern Ocean, *Ant. Sci.*, *16*(4), 471-486.

Arrigo, K. R. and G. L. van Dijken (2003), Phytoplankton dynamics within 37 Antarctic coastal polynyas, *J. Geophys. Res.*, *108*(C8), 3271, 10.1029/2002JC001739.

Arrigo, K. R. and G. L. van Dijken (2004), Annual changes in sea ice, chlorophyll *a*, and primary production in the Ross Sea, Antarctica, *Deep-Sea Res., Part II*, *51*, 117-138.

Arrigo, K. R., and G. L. Van Dijken (2007), Interannual variation in air-sea CO_2 flux in the Ross Sea, Antarctica: A model analysis, *J. Geophys. Res.*, *112*, C03020, doi:10.1029/2006JC003492.

Arrigo, K. R., C. W. Sullivan, and J. N. Kremer (1991), A bio-optical model of Antarctic sea ice, *J. Geophys. Res.*, *96*, 10581-10592.

Arrigo, K. R., D. L. Worthen, A. Schnell, and M. P. Lizotte (1998a), Primary production in Southern Ocean waters, *J. Geophys. Res.*, *103*, 15,587-15,600.

Arrigo, K. R., D. H. Robinson, M. P. Lizotte, D. L. Worthen, and B. Schieber (1998b), Bio-optical properties of the southwestern Ross Sea, *J. Geophys. Res*., *103*, 21,683-21,695.

Arrigo, K. R., G. R. DiTullio, R. B. Dunbar, M. P. Lizotte, D. H. Robinson, M. VanWoert, and D. L. Worthen (2000), Phytoplankton taxonomic variability and nutrient utilization and primary production in the Ross Sea, *J. Geophys. Res*., *105*, 8827-8846.

Arrigo, K. R., D. H. Robinson, R. B. Dunbar, A. R. Leventer, and M. P. Lizotte (2003) Physical control of chlorophyll *a*, POC, and PON distributions in the pack ice of the Ross Sea, Antarctica, *J. Geophys. Res*., *108*(C10), 3316, 10.1029/2001JC001138.

Barbini, R., F. Colao, R. Fantoni, L. Fiorani, N. V. Kolodnikova, and A. Palucci (2006), A Laser remote sensing calibration of ocean color satellite data, *Annals Geophys*., *49*(1), 35-43.

Becquevort, S., and W. O. Smith, Jr. (2001), Aggregation, sedimentation and biodegradability of phytoplankton-derived material during spring in the Ross Sea, Antarctica, *Deep-Sea Res., Part II*, *48*, 4155-4178.

Behrenfeld, M. J. and P. G. Falkowski (1997), Photosynthetic rates derived from satellite-based chlorophyll concentration, *Limnol. Oceanogr*., *42*(1), 1-20.

Behrenfeld, M. J., R. T. O'Malley, D. A. Siegel, C. R. McClain, J. L. Sarmiento, G. C. Feldman, A. J. Milligan, P. G. Falkowski, R. M. Letelier, and E. S. Boss. (2006), Climate-driven trends in contemporary ocean productivity, *Nature*, *444*(7120), 752-755.

Boyd, P.W., A.J. Watson, C.S. Law, E.R. Abraham, T. Trull, R. Murdoch, D.C. E. Bakker, A.R. Bowie, K.O. Buessler, H. Chang, M.A. Charette, P. Croot, K. Downing, R.D. Frew, M. Gall, M. Hadfield, J.A. Hall, M. Harvey, G. Jameson, J. La Roche, M.I. Liddicoat, R. Ling, M. Maldonado, R.M. McKay, S.D. Nodder, S. Pickmere, R. Pridmore, S. Rintoul, K. Safi, P. Sutton, R. Strzepek, K. Tanneberger, S.M. Turner, A. Waite, and J. Zeldis (2000), A mesoscale phytoplankton bloom in the polar Southern Ocean stimulated by iron fertilization, *Nature*, *407*, 695-702.

Broecker, W. S. (1991), The great ocean conveyor, *Oceanography*, *4*, 79-89.

Caldeira, K, and P.B. Duffy (2000), The role of the Southern Ocean in uptake and storage of anthropogenic carbon dioxide, *Science*, *287*, 620-622.

Carr, M-.E., M. A. M. Friedrichs, M. Schmeltz, M. N. Aita, D. Antoine, K. R. Arrigo, I. Asanuma, O. Aumont, R. Barber, M. Behrenfeld, R. Bidigare, E. Bustenhuis, J. Campbell, A. Ciotti, H. Dierssen, M. Dowell, J. Dunne, W. Esaias, B. Gentili, S. Grom, N. Hoepffner, J. Ishizaka, T. Kameda, C. LeQuére, S. Lohrenz, J. Marra, F. Mélin, K. Moore, A. Morel, T. Reddy, J. Ryan, M. Scardi, T. Smyth, K. Turpie, G. Tilstone, K. Waters, and Y. Yamanaka (2006), A comparison of global estimates of marine primary production from ocean color, *Deep-Sea Res., Part II*, 53(5-7), 741-770.

Coale, K. H., K. S. Johnson, F. P. Chavez, K. O. Buesseler, R. T. Barber, M. A. Brzezinski, W. P. Cochlan, F. J. Millero, P. G. Falkowski, J. E. Bauer, et. al. (2002), Southern Ocean iron enrichment experiment: carbon cycling in high- and low-Si waters, *Science*, *304*(5669), 408-414.

Cochlan, W. P., D. A. Bronk, and K. H. Coale (2002), Trace metals and nitrogenous nutrition of Antarctic phytoplankton: experimental observations in the Ross Sea, *Deep-Sea Res., Part II*, *49*, 3365-3390.

Dennett, M. R., S. Mathot, D. A. Caron, W. O. Smith, Jr., and D. J. Lonsdale (2001), Abundance and distribution of phototrophic and heterotrophic nano- and microplankton in the southern Ross Sea, *Deep-Sea Res., Part II*, *48*, 4019-4037.

Dobson, F. W. and S. D. Smith (1988), Bulk models of solar radiation at sea, *Q. J. R. Meteorol. Soc., 114*, 165-182.

Ducklow, H. W., W. Fraser, D. M. Karl, L. B. Quetin, R. M. Ross, R. C. Smith, S. E. Stammerjohn, M. Vernet, and R. M. Daniels (2006), Water-column processes in the West Antarctic Peninsula and the Ross Sea: Interannual variations and foodweb structure, *Deep-Sea Res., Part II*, *53*(8-10) 834-852.

Eppley, R.W. (1972), Temperature and phytoplankton growth in the sea, *Fish. Bull.*, *70*, 1063-1085.

Fennel, K., M. R. Abbott, Y. H. Spitz, J. G. Richman, and D. M. Nelson (2003), Impacts of iron control on phytoplankton production in the modern and glacial Southern Ocean, *Deep-Sea Res., Part II*, *50*(3-4), 833-851.

Fitch, D. T, and J. K. Moore (2007), Wind speed influence on phytoplankton bloom dynamics in the Southern Ocean Marginal Ice Zone, *J. Geophys. Res*., *112*, XXXXX, doi:10.1029/2006JC004061.

Gabric, A. J., R. Cropp, G. P. Ayers, G. McTainsh, and R. Braddock (2002), Coupling between cycles of phytoplankton biomass and aerosol optical depth as derived from SeaWiFS time series in the Subantarctic Southern Ocean, *Geophys. Res. Lett*., *29*(7), 16-1-4.

Garcia, C. A. E., V. M. T. Garcia, and C. R. McClain (2005), Evaluation of SeaWiFS chlorophyll algorithms in the Southwestern Atlantic and Southern Oceans, *Remote Sens. Env*., *95*(1), 125-137.

Gervais, F., U. Riebesell, and M. Y. Gorbunov (2002), Changes in primary productivity and chlorophyll *a* in response to iron fertilization in the Southern Polar Frontal Zone, *Limnol. Oceanogr*., *47*(5), 1324-1335.

Gibson, J. A. E. and T. W. Trull (1999), Annual cycle of fCO_2 under sea-ice and in open water in Prydz Bay, East Antarctica, *Mar. Chem*., *66*(3-4), 187-200.

Gowing, M. M., D. L. Garrison, H. B. Kunze, and C. J. Winchell (2001), Biological components of Ross Sea short-term particle fluxes in the austral summer of 1995-1996, *Deep-Sea Res., Part II*, *48*, 2645-2671.

Gradinger, R. R., and M. E. M. Baumann (1991), Distribution of phytoplankton communities in relation to the large-scale hydrographical regime in the Fram Strait, *Mar. Biol*., *111*, 311-321.

Gregg, W. W., and K. L. Carder (1990), A simple spectral solar irradiance model for cloudless maritime atmospheres, *Limnol. Oceanogr*., *35*, 1657-1675.

Hense, I., U.V. Bathmann, and R. Timmermann (2000), Plankton dynamics in frontal systems of the Southern Ocean, *J. Mar. Sys*., *27*(1-3), 235-252.

Holm-Hansen, O., M. Kahru, C. D. Hewes, S. Kawaguchi, T. Kameda, V. A. Sushin, I. Krasovski, J. Priddle, R. Korb, R. P. Hewitt, and B. G. Mitchell (2004), Temporal and spatial distribution of chlorophyll-a in surface waters of the Scotia Sea as determined by both shipboard measurements and satellite data, *Deep-Sea Res., Part II*, *51*(12-13), 1323-1331.

Kalnay, E., M. Kanamitsu, R. Kistler, W. Collins, D. Deaven, L. Gandin, M. Iredell, .S Saha, G. White, J. Woollen, Y. Zhu, M. Chelliah, W. Ebisuzaki, W. Higgins, J. Janowiak, K. C. Mo, C. Ropelewski, J. Wang, A. Leetmaa, R. Reynolds, R. Jenne, and D. Joseph (1996), The NCEP/NCAR 40-year reanalysis project, *Bull. Amer. Meteor. Soc*., *77*(3), 437-471.

Kattner, G., and G. Budeus (1997), Nutrient status of the Northeast Water Polynya, *J. Mar. Sys*., *10*, 185-197.

Kopczynska, E. E., L. Goeyens, M. Semeneh, and F. Dehairs (1995), Phytoplankton composition and cell carbon distribution in Prydz Bay, Antarctica: Relation to organic particulate matter and its delta-C-13 values, *J. Plankt. Res*., *17*, 685-707.

Korb, R. E. and M. Whitehouse (2004), Contrasting primary production regimes around South Georgia, Southern Ocean: Large blooms versus high nutrient, low chlorophyll waters, *Deep-Sea Res., Part I*, *51*(5), 721-738.

Korb, R. E., M. J. Whitehouse, and P. Ward (2004), SeaWiFS in the Southern Ocean: Spatial and temporal variability in phytoplankton biomass around South Georgia, *Deep-Sea Res., Part II*, *51*(1-3), 99-116.

Lancelot, C. C. Veth, and S. Mathot (1991), Modelling ice-edge phytoplankton bloom in the Scotia-Weddell sea sector of the Southern Ocean during spring 1998, *J. Mar. Sys*., *2*, 333-346.

Le Quéré, C., C. Röedenbeck, E.T. Buitenhuis, T. J. Conway, R. Langenfelds, A. Gomez, C. Labuschagne, M. Ramonet, T. Nakazawa, N. Metzl, and N. Gillett, and M. Heimann (2007), Saturation of the Southern Ocean CO_2 sink due to recent climate change, *Science*, *316*(5832), 1735-1738.

Lo Monaco, C., N. Metzl, A. Poisson, C. Brunet, and B. Schauer (2005), Anthropogenic CO_2 in the Southern Ocean: Distribution and inventory at the Indian-Atlantic boundary (World Ocean Circulation Experiment line I6), *J. Geophys Res*., *110*, C06010, doi:10.1029/2004JC002643.

Lomas, M. W. and N. R. Bates (2004), Potential controls on interannual partitioning of organic carbon during the winter/spring phytoplankton bloom at the Bermuda Atlantic Time-series Study (BATS) site, *Deep-Sea Res., Part I*, *51*(11), 1619-1636.

Longhurst, A., S. Sathyendranath, T. Platt and C. Caverhill (1995), An estimate of global primary production in the ocean from satellite radiometer data, *J. Plankton Res*., *17*, 1245-1271.

Louanchi, F., M. Hoppema, D. C. E. Bakker, A. Poisson, M. H. C. Stoll, H. J. W. De Baar, B. Schauer, D. P. Ruiz-Pino, and D. Wolf-Gladrow (1999a), Modelled and observed sea surface fCO_2 in the southern ocean: a comparative study, *Tellus Series B*, *51*(2), 541-559.

Louanchi, F., D. P. Ruiz-Pino, and A. Poisson (1999b), Temporal variations of mixed-layer oceanic CO_2 at JGOFS-KERFIX time-series station: Physical versus biogeochemical processes, *J. Mar. Res*., *57*(1), 165-187.

Lovenduski, N S. and N. Gruber (2005), Impact of the Southern Annular Mode on Southern Ocean circulation and biology, *Geophys. Res. Lett.*, *32*(11), 1-4.

Markus, T. and B. A. Burns (1995), A method to estimate subpixel-scale coastal polynyas with satellite passive microwave data, *J. Geophys. Res*., *100*, 4473-4487.

Marrari, M., C.M. Hu, K. Daly (2006), Validation of SeaWiFS chlorophyll *a* concentrations in the Southern Ocean: A revisit, *Remote Sens. Env*. *105*(4), 367-375.

Martin, J. H. (1990), Glacial-interglacial CO_2 change: The iron hypothesis, *Paleoceanogr.*, *5*, 1-13.

McClain, C. R., K. R., Arrigo, K.-S. Tai, and D. Turk (1996), Observations and simulations of physical and biological processes at OWS P, 1951-1980, *J. Geophys. Res., 101*, 3697-3713.

McNeil, B. I., B. Tilbrook, R. J. Matear (2001), Accumulation and uptake of anthropogenic CO_2 in the Southern Ocean, south of Australia between 1968 and 1996, *J. Geophys. Res., 106*(C12), 31431-31445.

Meehl, G.A., W.D. Collins, B.A. Boville, J.T. Kiehl, T.M.L. Wigley, and J.M. Arblaster (2000), Response of the NCAR climate system model to increased CO_2 and the role of physical processes, *J. Climate*, *13*(11), 1879-1898.

Mitchell, B.G. and O. Holm-Hansen (1991), Bio-optical properties of Antarctic Peninsula waters: differentiation from temperate ocean models, *Deep-Sea Res*., *Part A*, *38*, 1009-1028.

Moore, J. K. and M. R. Abbott (2000), Phytoplankton chlorophyll distributions and primary production in the Southern Ocean, *J. Geophys. Res., 105*(C12), 28709-28722.

Morel, A. (1978), Available, usable, and stored radiant energy in relation to marine photosynthesis, *Deep-Sea Res.*, *25*, 673-688.

O'Reilly, J., S. Maritorena, B. G. Mitchell, D. A. Siegel, K. L. Carder, M. Kahru, S. A. Garver, and C. R. McClain (1998), Ocean color algorithms for SeaWiFS. *J. Geophys. Res.*, *103*, 24,937–24,953.

Pope, R.M. and E.S. Fry (1997), Absorption spectrum (380-700 nm) of pure water. II. Integrating cavity measurements, *Appl. Opt*., *36*, 8710-8723.

Reuer, M. K., B. A. Barnett, M. L. Bender, P. G. Falkowski, M. B. Hendriks (2007), New estimates of Southern Ocean biological production rates from O2/Ar ratios and the triple isotope composition of O2, *Deep-Sea Res., Part I*, *54*, 951-974.

Rey, F., T. T. Noji, and L. A. Miller (2000), Seasonal phytoplankton development and new production in the central Greenland Sea, *Sarsia*, *85*, 329-344.

Reynolds, R.W., N.A. Rayner, T.M. Smith, D.C. Stokes, and W. Wang (2002), An improved in situ and satellite SST analysis for climate. *J. Climate*, *15*, 1609-1625.

Rind, D., R. Healy, C. Parkinson, and D. Martinson (1997), The role of sea ice in $2xCO_2$ climate model sensitivity. 2. Hemispheric dependencies, *Geophys. Res. Lett.*, *24*(12), 491-1494.

Russell, J.L., R.J. Souffer, and K.W. Dixon (2006a), Intercomparison of the Southern Ocean Circulations in the IPCC Coupled Model Control Simulations, *J. Climate*, *19*(18), 4560-4575.

Russell, J.L., K.W. Dixon, A. Gnanadesikan, R.J. Stouffer, and J.R. Toggweiler (2006b), The Southern Hemisphere Westerlies in a Warming World: Propping Open the Door to the Deep Ocean, *J. Climate*, *19*(24), 6382-6390.

Sabine, C. L., R. A. Feely, R. M. Key, J. L. Bullister, F. J. Millero, K. Lee, T. H. Peng, B. Tilbrook, T. Ono, and C. S. Wong (2002), Distribution of anthropogenic CO_2 in the Pacific Ocean, *Global Biogeochem. Cycles*, *16*(4), 1083-1083.

Sarmiento, J.L., T.M.C. Hughes, R.J. Stouffer, and S. Manabe (1998). Simulated response of the ocean carbon cycle to anthropogenic climate warming, *Nature*, *393*, 245-249.

Sarmiento, J. L., N. Gruber, M. A. Brzezinski, and J. P. Dunne (2004), High-latitude controls of thermocline nutrients and low latitude biological productivity, *Nature*, *427*, 56-60.

Skogen, M. D. and A. Moll (2000), Interannual variability of the North Sea primary production: comparison from two model studies, *Cont. Shelf Res*., *20*(2), 129-151.

Smith, R.C. and K.S. Baker (1981), Optical properties of the clearest natural waters (200-800 nm), *Appl Opt*., *20*(2), 177-184.

Smith, W. O. Jr. (1995), Primary productivity and new production in the Northeast Water (Greenland) polynya during summer-1992, *J. Geophys. Res*., *100*, 4357-4370.

Smith Jr., W. O., Jr. and D. M. Nelson (1986), Importance of ice-edge phytoplankton production in the Southern Ocean, *BioScience*, *36*, 251-256.

Smith, W. O., Jr. and L. I. Gordon (1997), Hyperproductivity of the Ross Sea (Antarctica) polynya during austral spring, *Geophys. Res. Lett*., *24*, 233-236.

Steinberg, D.K., C.A. Carlson, N.R. Bates, R.J. Johnson, A.F. Michaels, and A. H. Knap (2001), Overview of the US JGOFS Bermuda Atlantic Time-series Study (BATS): a decade-scale look at ocean biology and biogeochemistry, *Deep-Sea Res., Part II*, *48*, 1405-1447.

Sullivan, C. W., K. R. Arrigo, C. R. McClain, J. C. Comiso, J. Firestone (1993), Distributions of phytoplankton blooms in the Southern Ocean, *Science*, *262*, 1832-1837.

Sweeney, C. (2003), The annual cycle of surface water CO_2 and O_2 in the Ross Sea: A model for gas exchange on the continental shelves of Antarctica, in *Biogeochemistry of the Ross Sea*, R. Dunbar and G. DiTullio (Eds), *Ant. Res. Ser.*, *78*, 295-312.

Takahashi, T., S. C. Sutherland, C. Sweeney, A. Poisson, N. Metzl, B. Tilbrook, N. Bates, R. Wanninkhof, R. A. Feely, C. Sabine, J. Olafsson, and Y. Nojiri (2002), Global sea-air CO_2 flux based on climatological surface ocean pCO_2, and seasonal biological and temperature effects, *Deep-Sea Res., Part II*, *49*(9-10), 601-1622.

Thompson D. W. J. and S. Solomon (2002), Interpretation of recent Southern Hemisphere climate change, *Science*, *296*, 895–899.

Turner, J., J. E. Overland, and J. E. Walsh (2007), An Arctic and Antarctic perspective on recent climate change, *Int. J. Clim*., *27*(3), 277-293.

von Quillfeldt, C. H. (1997), Distribution of diatoms in the Northeast Water Polynya, Greenland, *J. Mar. Sys*., *10*, 211-240.

Waugh, D. W., T. M. Hall, B. I. McNeil, R. Key, R. J. Matear (2006), Anthropogenic CO_2 in the oceans estimated using transit time distributions, *Tellus Series B*, *58*(5), 376-389.

Figure legends

Figure 1. Map of the study area showing the location of the five geographic sectors.

Figure 2. Maps showing how the four ecological provinces (pelagic, MIZ, shelf, and MIZ-shelf) used in the present study vary in size and location over time during the major phytoplankton growing season.

Figure 3. Locations in the Southern Ocean where Chl *a* samples used to validate the SeaWiFS OC4v4 algorithm were collected. The number of samples in a given location is given by the size and color of the triangles. Separate analyses were carried out for each of

the delineated regions. W/S = Weddell/Scotia Sea, RS = Ross Sea, PB = Prydz Bay, WAP = Western Antarctic Peninsula.

Figure 4. Relative frequency distributions for Chl *a* measured *in situ* and from SeaWiFS for a) all waters south of 50°S, b) the Western Antarctic Peninsula (WAP), c) deep waters of the Southern Ocean, d) the Ross Sea, e) the Weddell/Scotia Sea, and f) Prydz Bay. The boundaries of each region is given in Fig. 3.

Figure 5. Plots of primary production versus Chl *a* derived by the primary production algorithm and measured *in situ* at discrete stations near the a) Antarctic Peninsula (64°W-73°W, 64°S-68°S) and b) in the Ross Sea (165°E-165°W, 74°S-78°S). Algorithm output used in this analysis was restricted to those times and locations for which *in situ* data were available.

Figure 6. Annual cycles of open water area and spatially averaged daily primary production in the different ecological provinces of the Southern Ocean between 1997 and 2006.

Figure 7. Annual climatologies (1997-2006) used to calculate anomalies for a) sea ice cover, b) sea surface temperature, c) Chl *a*, and d) primary production.

Figure 8. Anomaly maps of annual primary production for each of the nine years of our study. Colors represent change from climatological mean shown in Fig. 16a.

Figure 9. Anomaly maps of Chl *a* for each of the nine years of our study. Colors represent change from climatological mean shown in Fig. 16b.

Figure 10. Anomaly maps of sea ice cover for each of the nine years of our study. Colors represent change from climatological mean shown in Fig. 16c.

Figure 11. Anomaly maps of sea surface temperature for each of the nine years of our study. Colors represent change from climatological mean shown in Fig. 16d.

Figure 12. Maps of the correlation coefficient between mean annual primary production and a) mean annual Chl *a*, b) mean annual sea ice cover, and c) mean annual sea surface temperature for the nine years of our study. Only pixel locations where data from all nine years are shown in color. Grey areas denote pixels where one or more years of

data are unavailable. Also shown (d) is a map of the ecological provinces on 11 December 1998 to illustrate that the position of the MIZ corresponds well with areas exhibiting a high positive correlation between mean annual sea ice cover and mean annual primary production (Fig. 21b).

Figure 13. Schematic representation of the variation by ecological province in the strength of the correlation between a) mean annual primary production and year, b) mean annual primary production and mean annual open water area, c) mean annual open water area and year, and d) mean annual primary production and the Southern Annular Mode. The locations of the ecological provinces shown in each panel (and defined in (a)) are highly idealized representations of their proximity to the coast.

Figure 14. Total annual primary production in the Southern Ocean between 1997 and 2006 plotted along with variability in the Southern Annular Mode (SAM) Index. Monthly SAM data were obtained from the NOAA Climate Prediction Center (http://www.cpc.noaa.gov/products/precip/CWlink/daily_ao_index/aao/aao_index.html) and smoothed using a 3-month moving average. Although the relationship between SAM and annual primary production is not significant (R^2=0.31, p=0.12), changes in both variables are quite similar.

Figure 15. Ratio of the maximum to the minimum open water area during 1997-2006 regressed against the ratio of the maximum to minimum annual production for each geographic sector and ecological province.

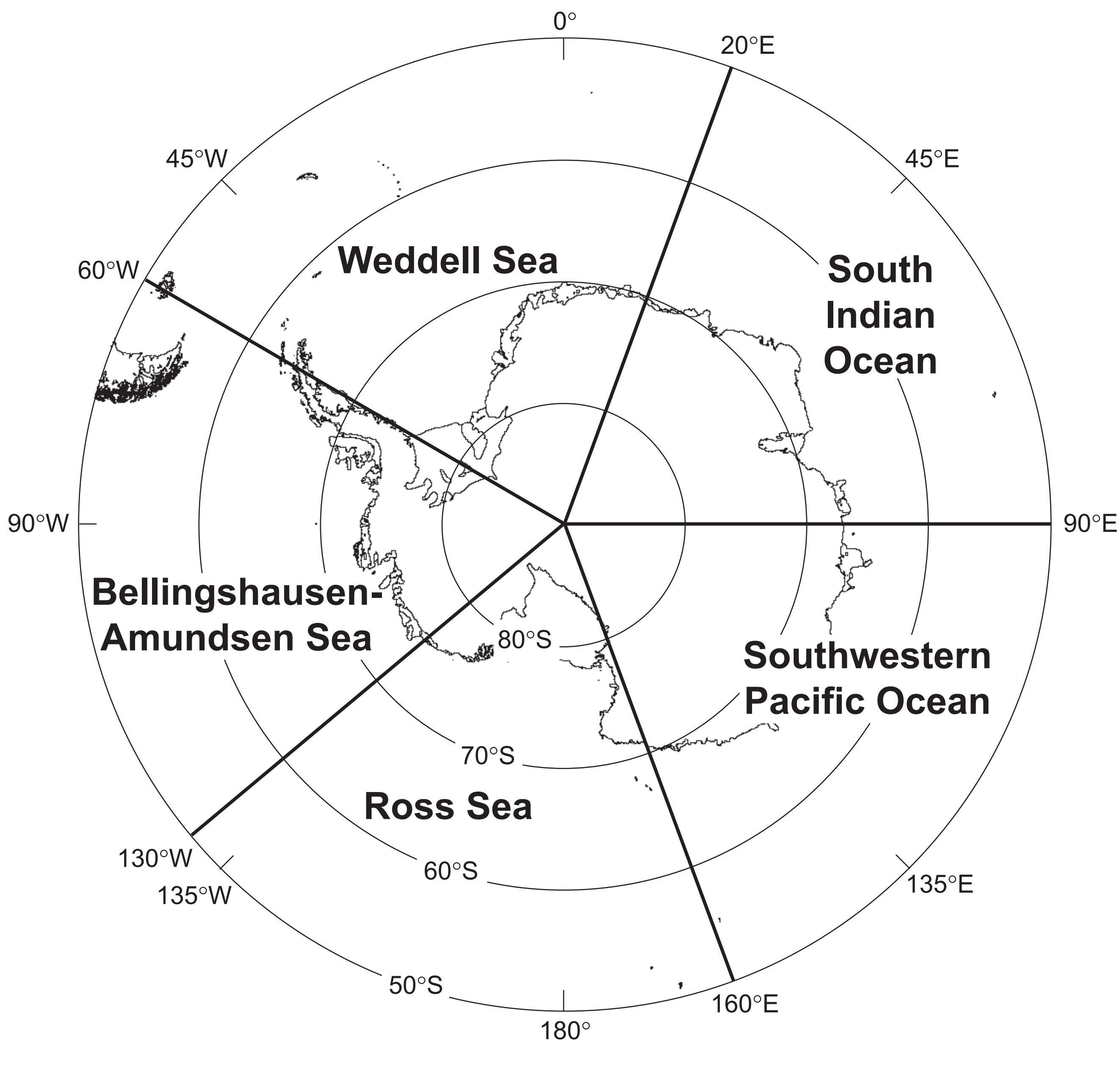
0°
20°E
45°W
45°E
60°W
Weddell Sea
South
Indian
Ocean
90°W
90°E
Bellingshausen-
Amundsen Sea
80°S
Southwestern
Pacific Ocean
70°S
Ross Sea
130°W
135°W
60°S
135°E
50°S
180°
160°E

Figure 1

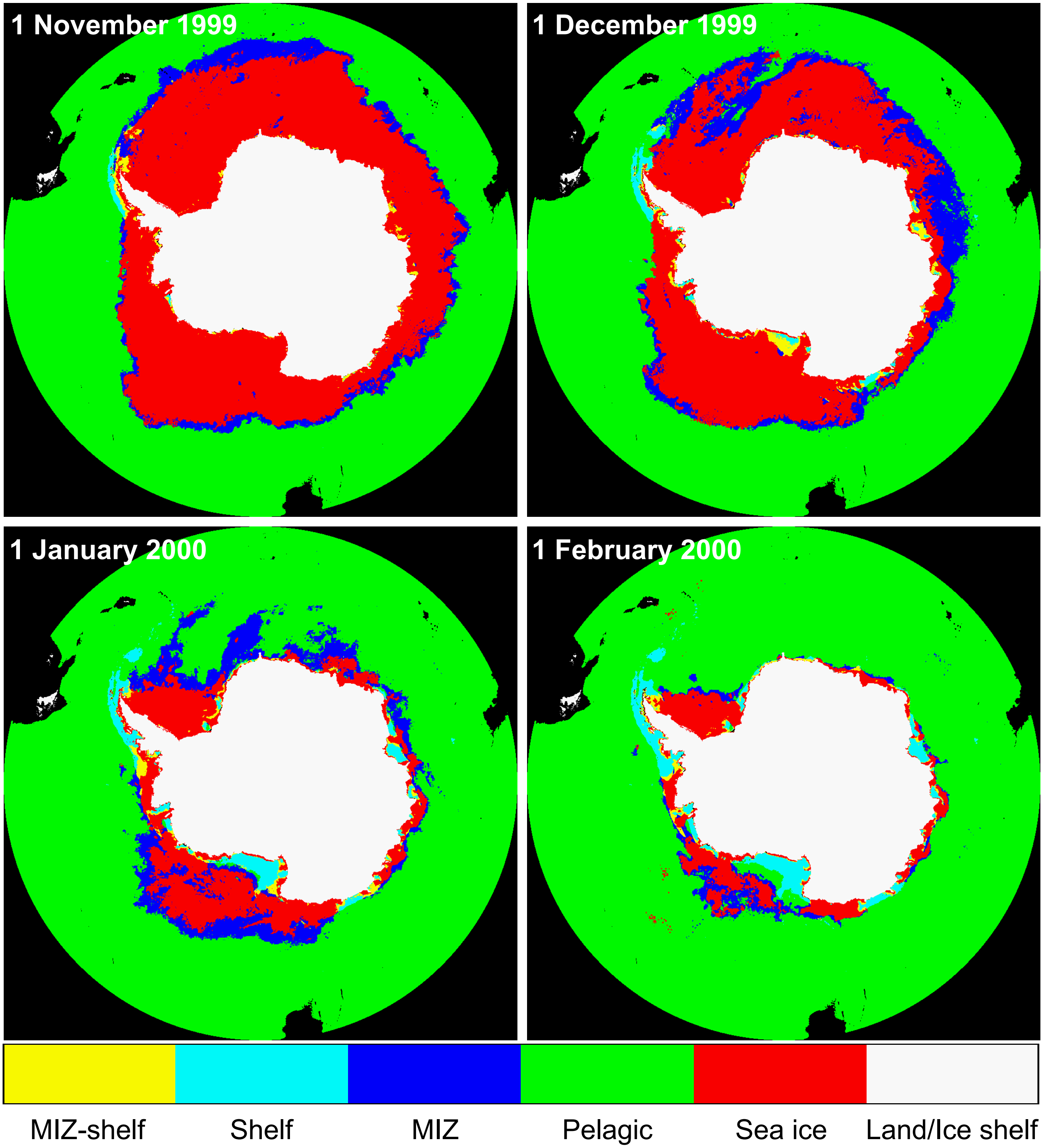
1 November 1999
1 December 1999
1 January 2000
1 February 2000
MIZ-shelf
Shelf
MIZ
Pelagic
Sea ice
Land/Ice shelf

Figure 2

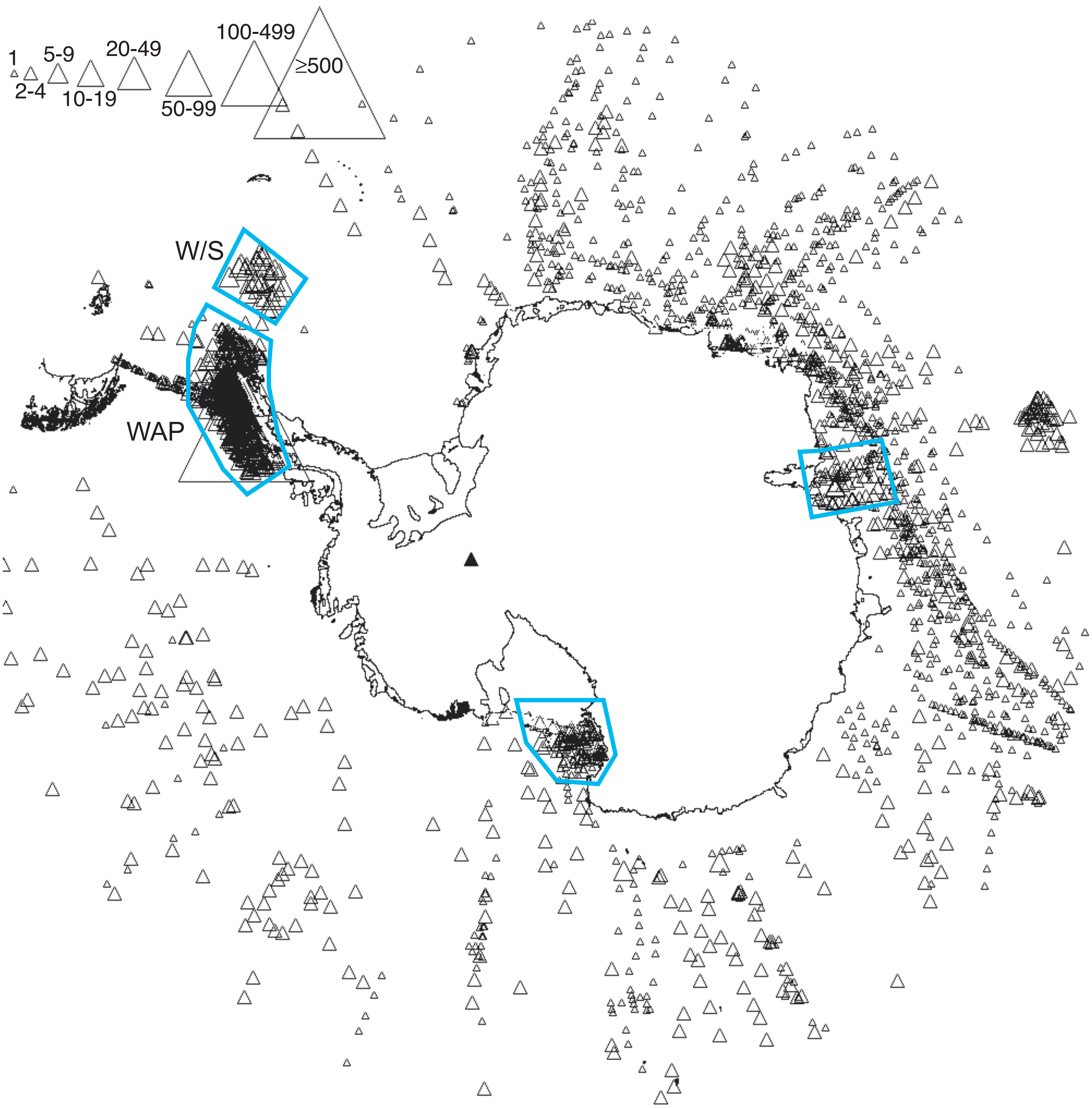

Figure 3

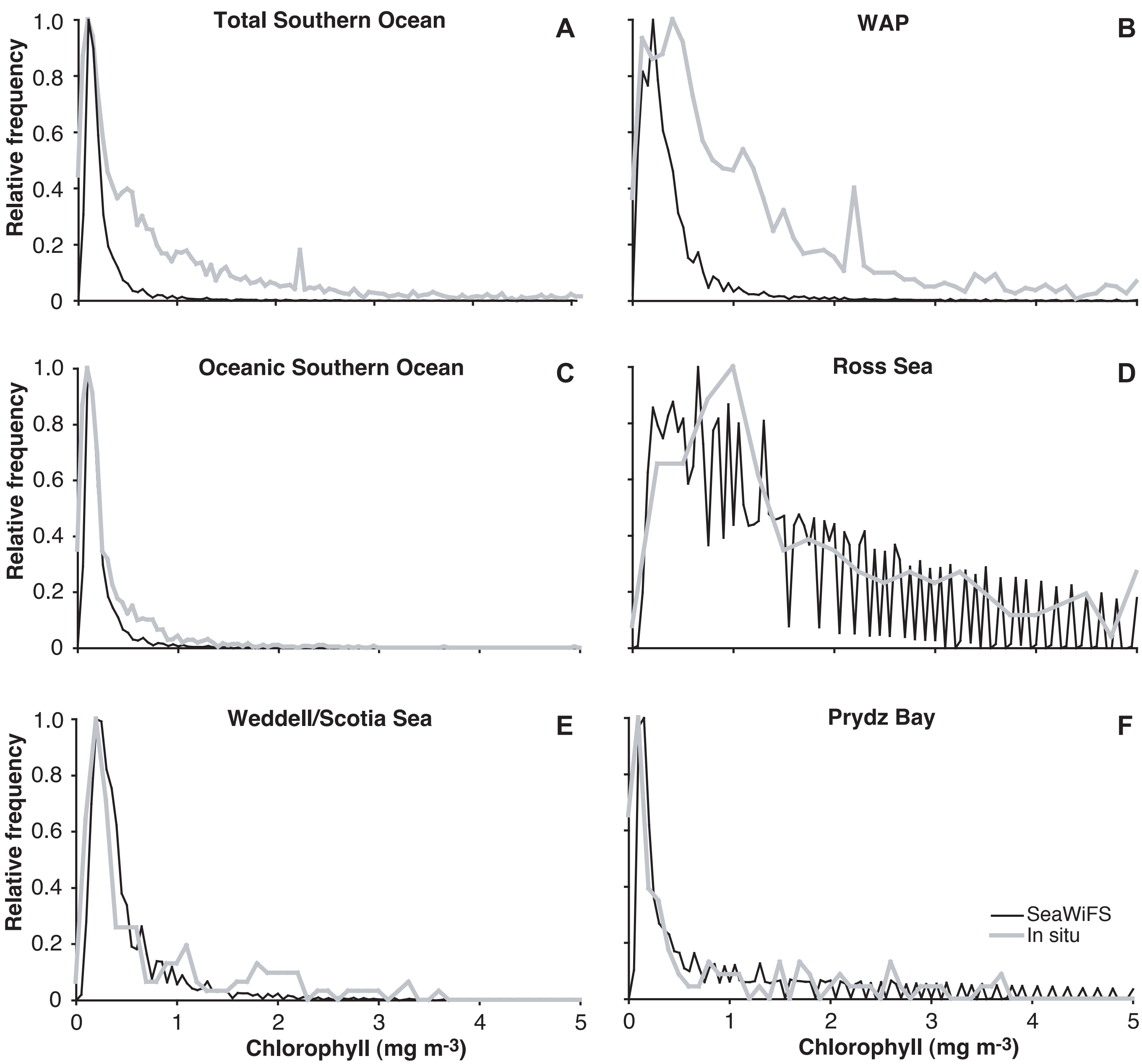
Total Southern Ocean
A
WAP
B
Oceanic Southern Ocean
C
Ross Sea
D
Weddell/Scotia Sea
E
Prydz Bay
F
Relative frequency
1.0
0.8
0.6
0.4
0.2
0
0
1
2
3
4
5
Chlorophyll (mg m-3)
SeaWiFS
In situ

Figure 4

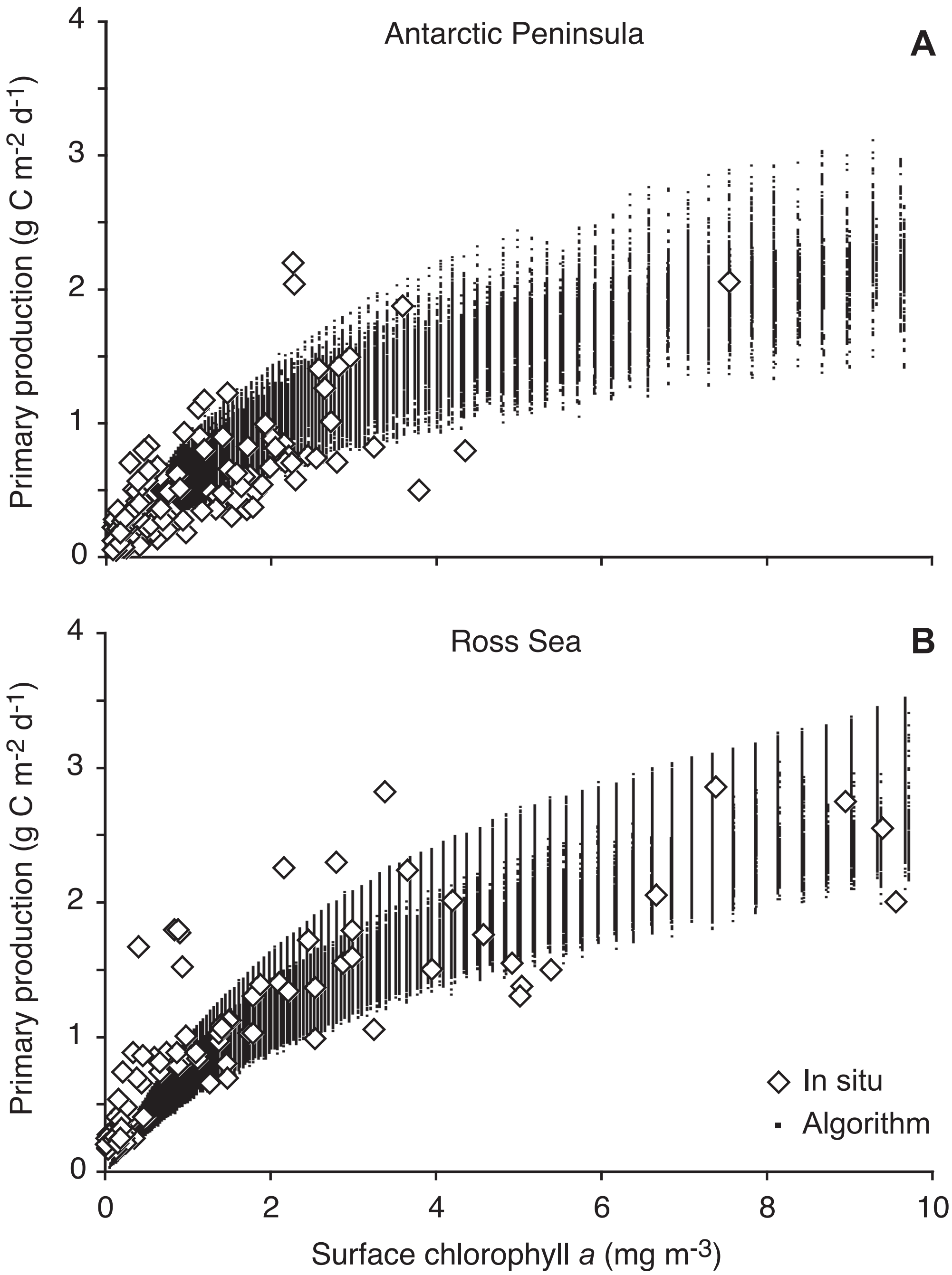
Antarctic Peninsula
A
Primary production (g C m-2 d-1)
Ross Sea
B
In situ
Algorithm
Surface chlorophyll a (mg m-3)
0
1
2
3
4
0
2
4
6
8
10

Figure 5

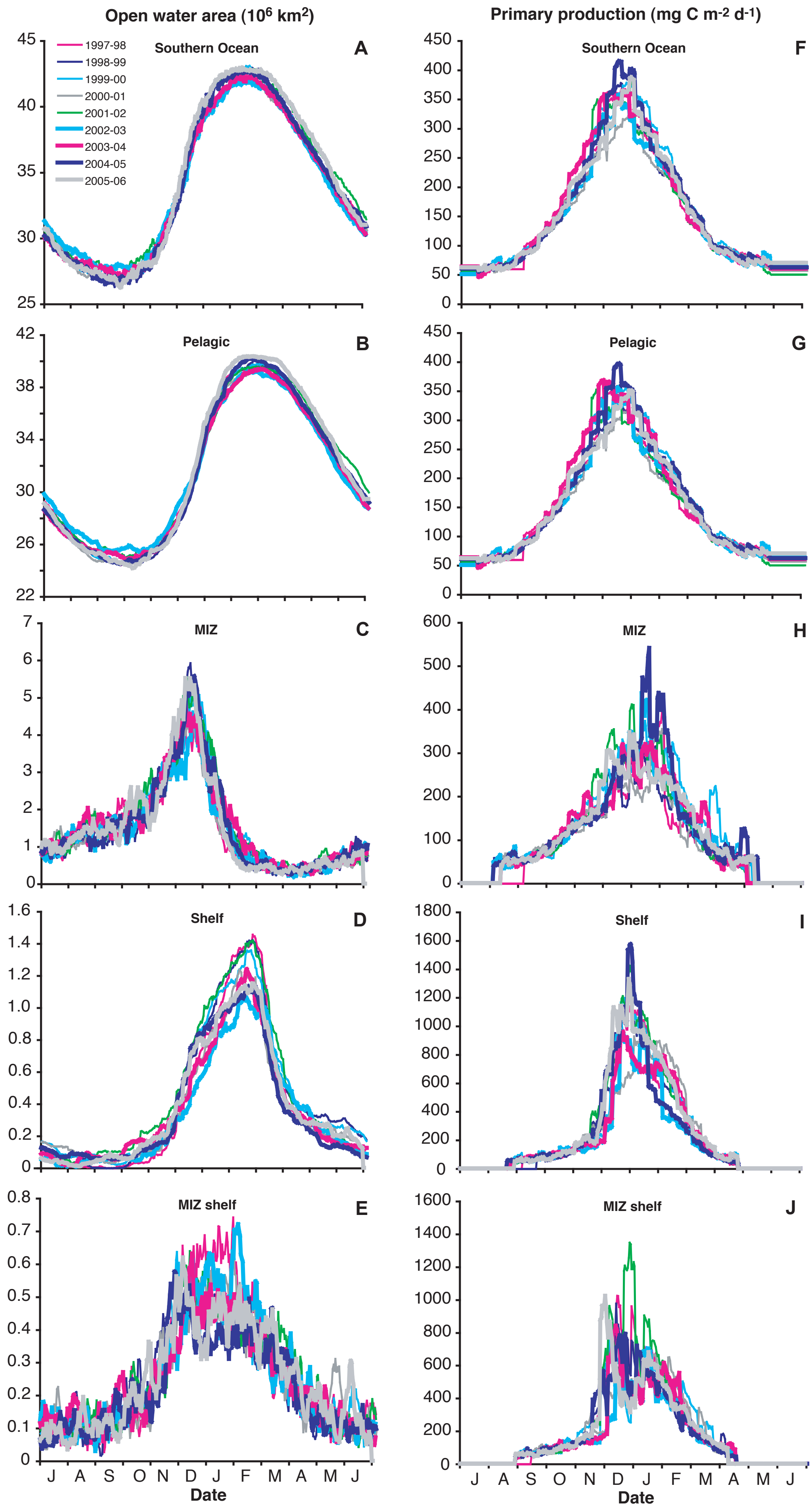
Open water area (10^6 km^2)
Primary production (mg C m^{-2} d^{-1})
1997-98
1998-99
1999-00
2000-01
2001-02
2002-03
2003-04
2004-05
2005-06
Southern Ocean
A
F
Pelagic
B
G
MIZ
C
H
Shelf
D
I
MIZ shelf
E
J
J A S O N D J F M A M J
Date

Figure 6

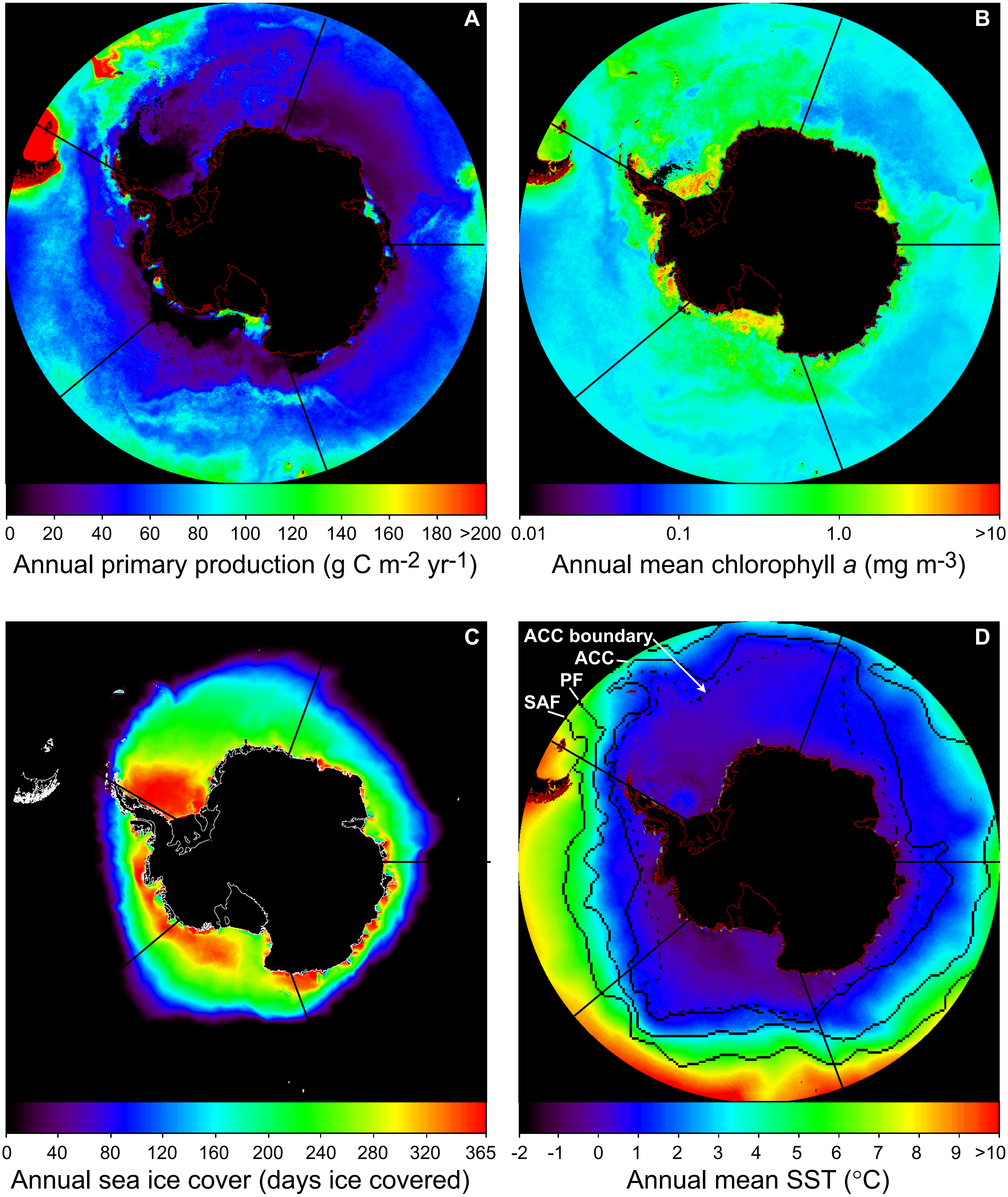
A
0 20 40 60 80 100 120 140 160 180 >200
Annual primary production (g C m-2 yr-1)
B
0.01 0.1 1.0 >10
Annual mean chlorophyll a (mg m-3)
C
0 40 80 120 160 200 240 280 320 365
Annual sea ice cover (days ice covered)
D
ACC boundary
ACC
PF
SAF
-2 -1 0 1 2 3 4 5 6 7 8 9 >10
Annual mean SST (°C)

Figure 7

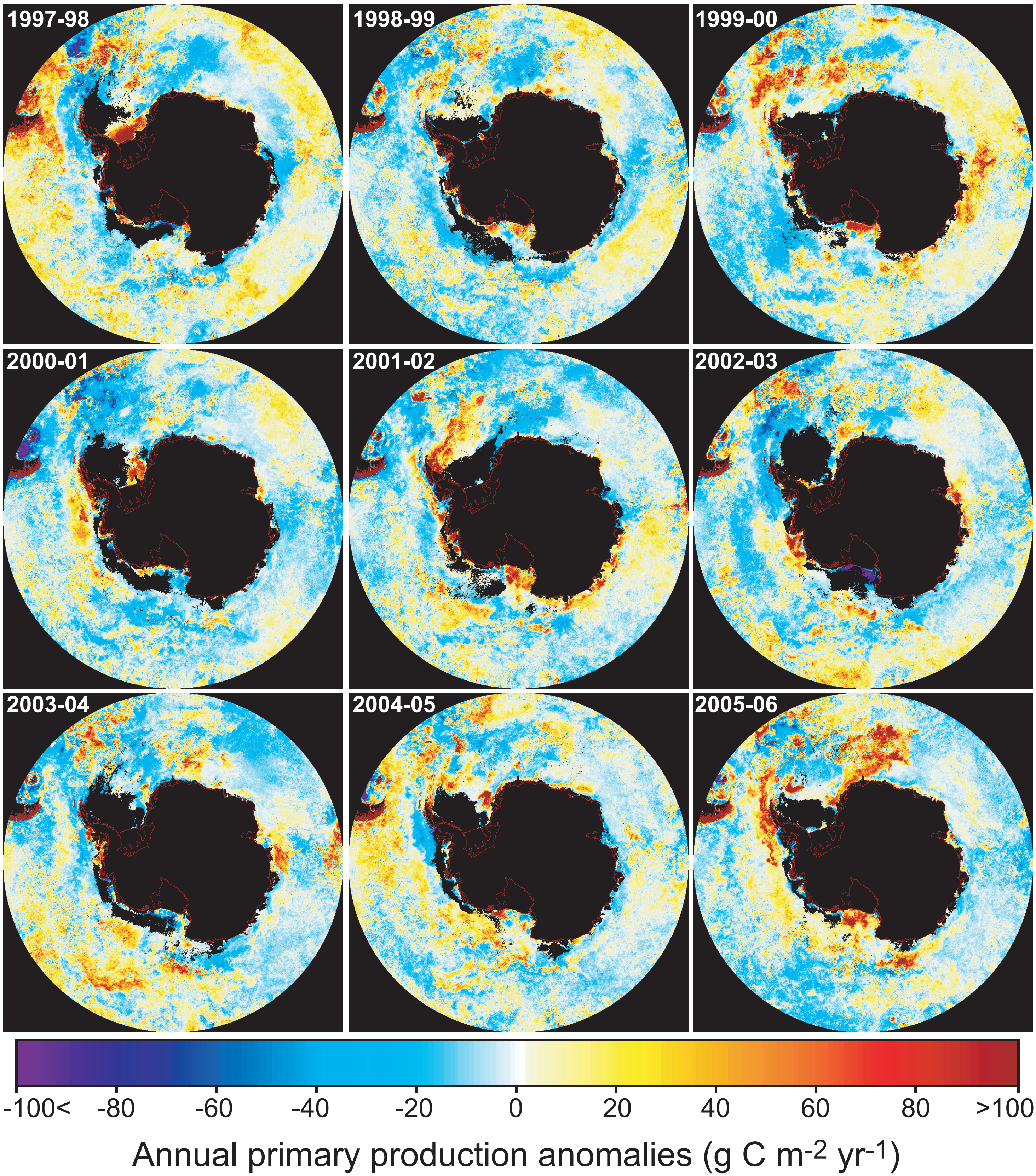
1997-98
1998-99
1999-00
2000-01
2001-02
2002-03
2003-04
2004-05
2005-06
-100< -80 -60 -40 -20 0 20 40 60 80 >100
Annual primary production anomalies (g C m-2 yr-1)

Figure 8

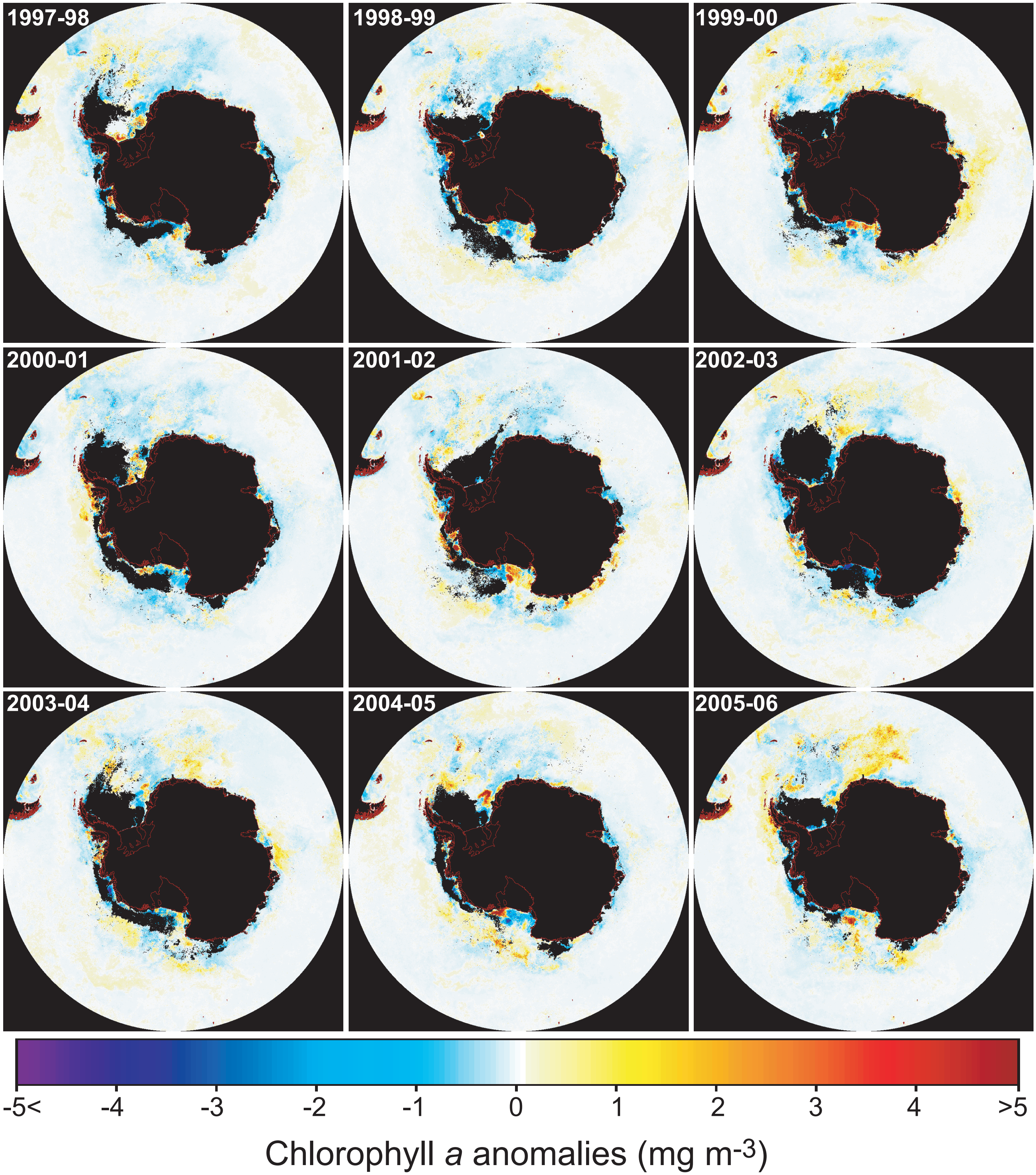
1997-98
1998-99
1999-00
2000-01
2001-02
2002-03
2003-04
2004-05
2005-06
-5<
-4
-3
-2
-1
0
1
2
3
4
>5
Chlorophyll *a* anomalies (mg m^{-3})

Figure 9

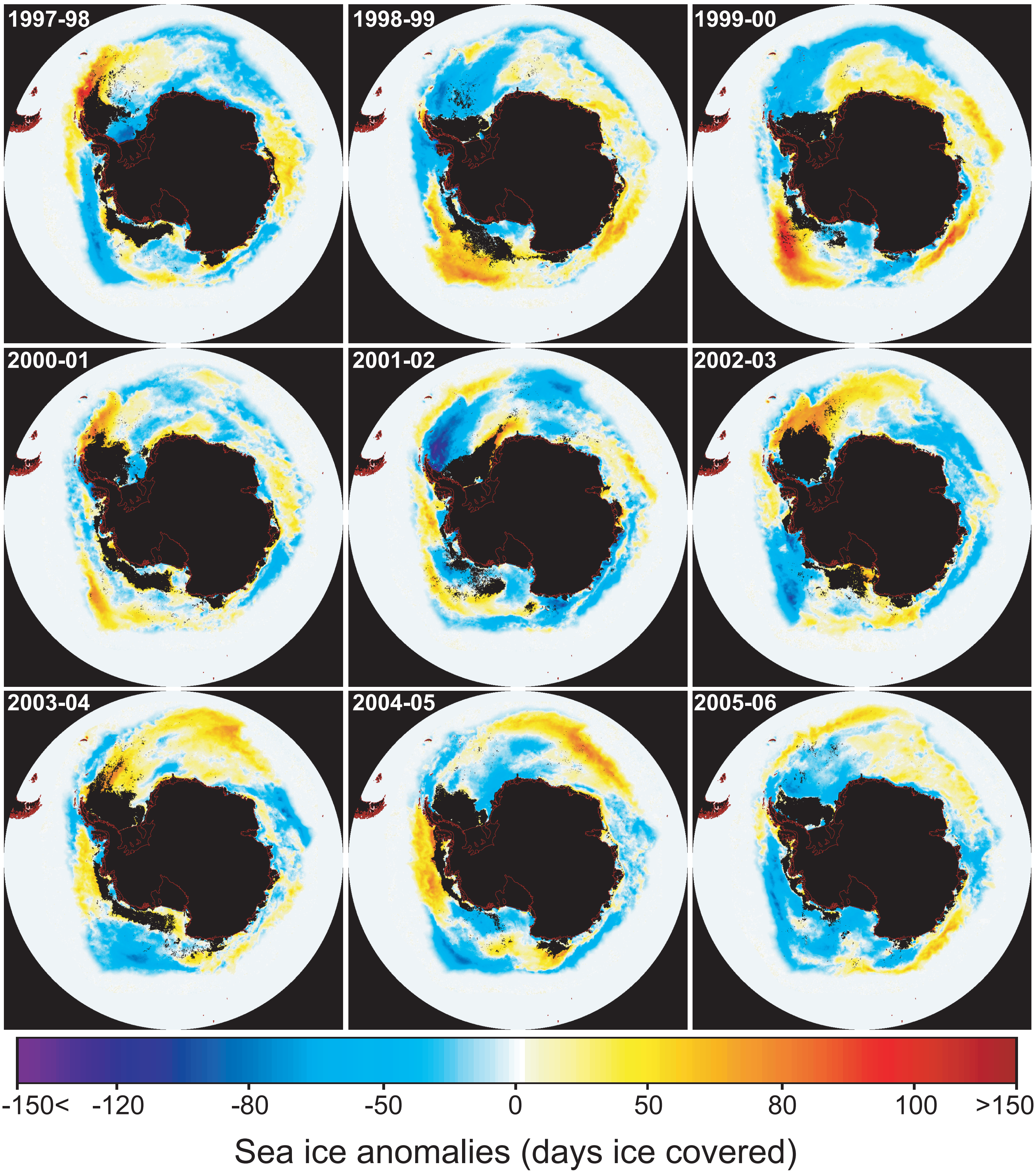
1997-98
1998-99
1999-00
2000-01
2001-02
2002-03
2003-04
2004-05
2005-06
-150<
-120
-80
-50
0
50
80
100
>150
Sea ice anomalies (days ice covered)

Figure 10

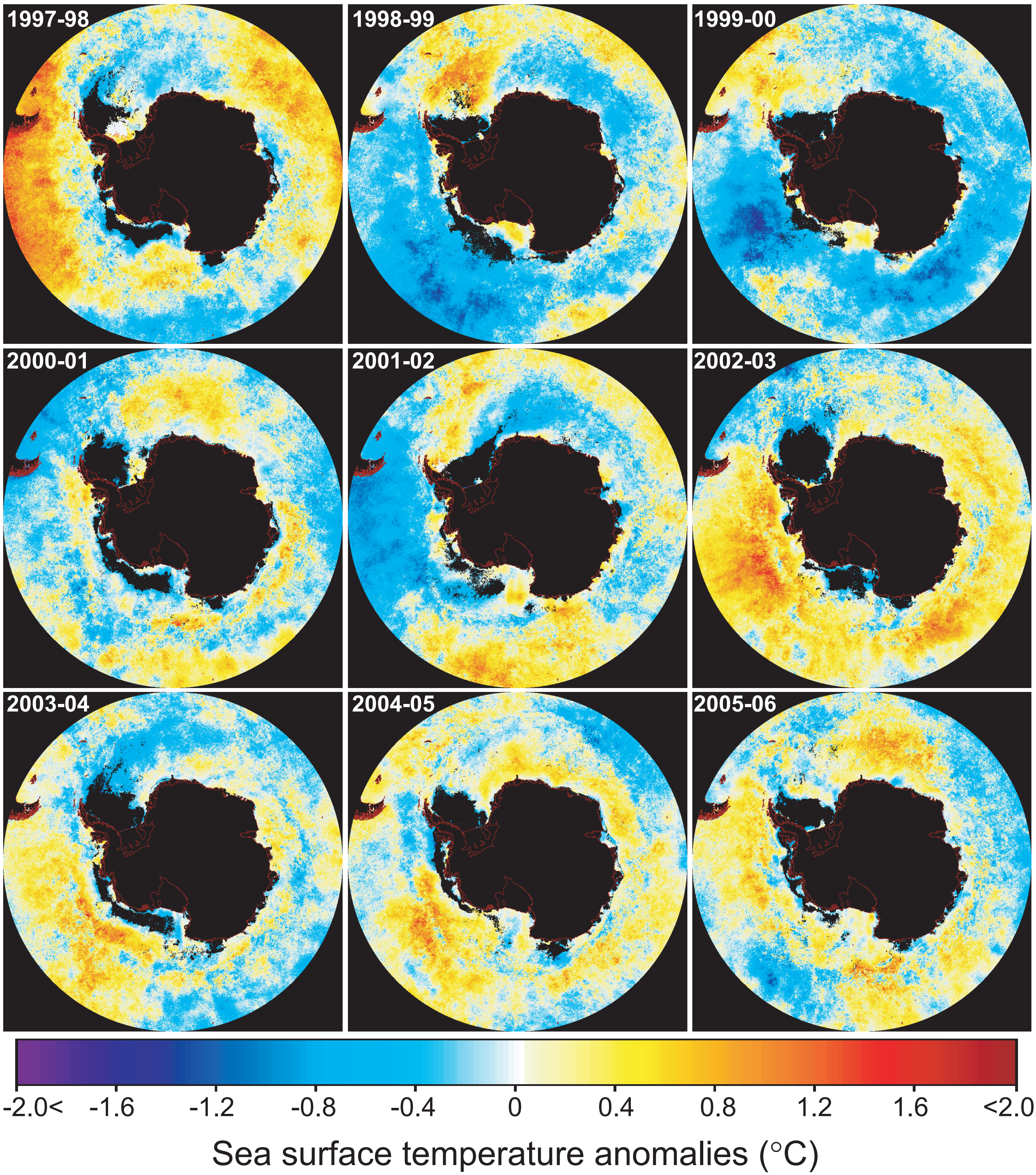
1997-98
1998-99
1999-00
2000-01
2001-02
2002-03
2003-04
2004-05
2005-06
-2.0< -1.6 -1.2 -0.8 -0.4 0 0.4 0.8 1.2 1.6 <2.0
Sea surface temperature anomalies (°C)

Figure 11

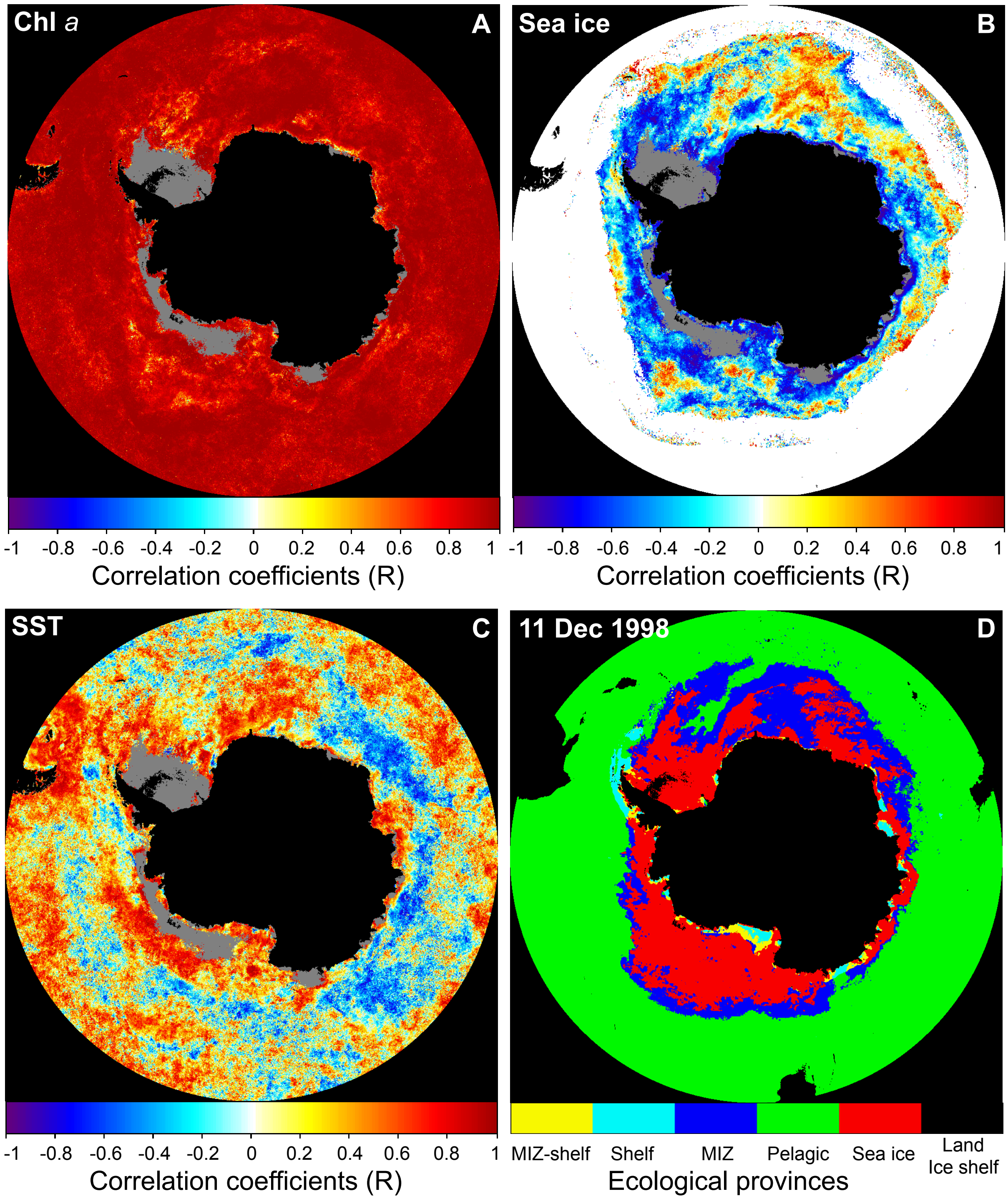

Chl a
A
Sea ice
B
-1 -0.8 -0.6 -0.4 -0.2 0 0.2 0.4 0.6 0.8 1
Correlation coefficients (R)
-1 -0.8 -0.6 -0.4 -0.2 0 0.2 0.4 0.6 0.8 1
Correlation coefficients (R)
SST
C
11 Dec 1998
D
-1 -0.8 -0.6 -0.4 -0.2 0 0.2 0.4 0.6 0.8 1
Correlation coefficients (R)
MIZ-shelf
Shelf
MIZ
Pelagic
Sea ice
Land
Ice shelf
Ecological provinces

Figure 12

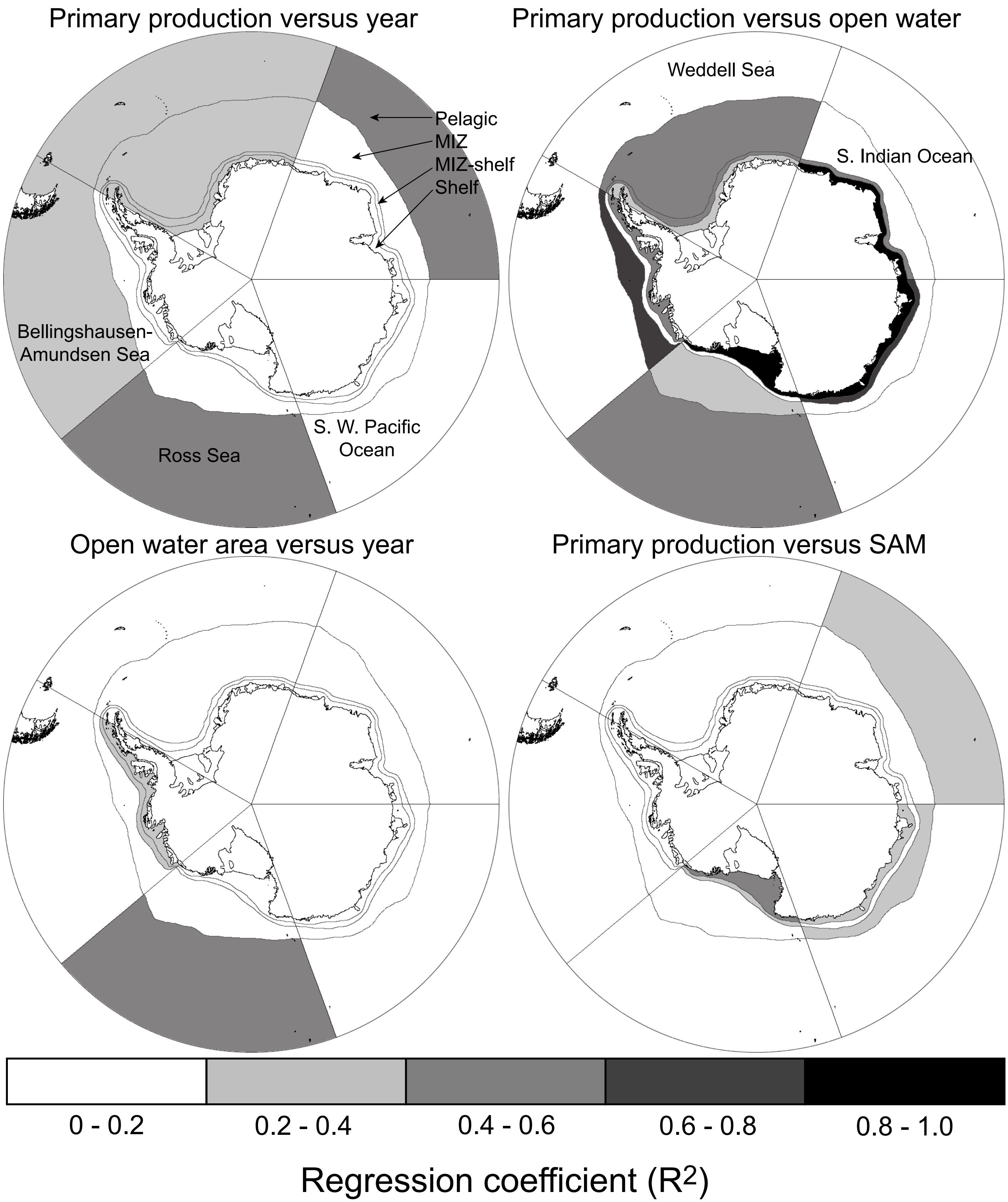

Primary production versus year
Pelagic
MIZ
MIZ-shelf
Shelf
Bellingshausen-Amundsen Sea
Ross Sea
S. W. Pacific Ocean
Primary production versus open water
Weddell Sea
S. Indian Ocean
Open water area versus year
Primary production versus SAM
0 - 0.2
0.2 - 0.4
0.4 - 0.6
0.6 - 0.8
0.8 - 1.0
Regression coefficient (R2)

Figure 13

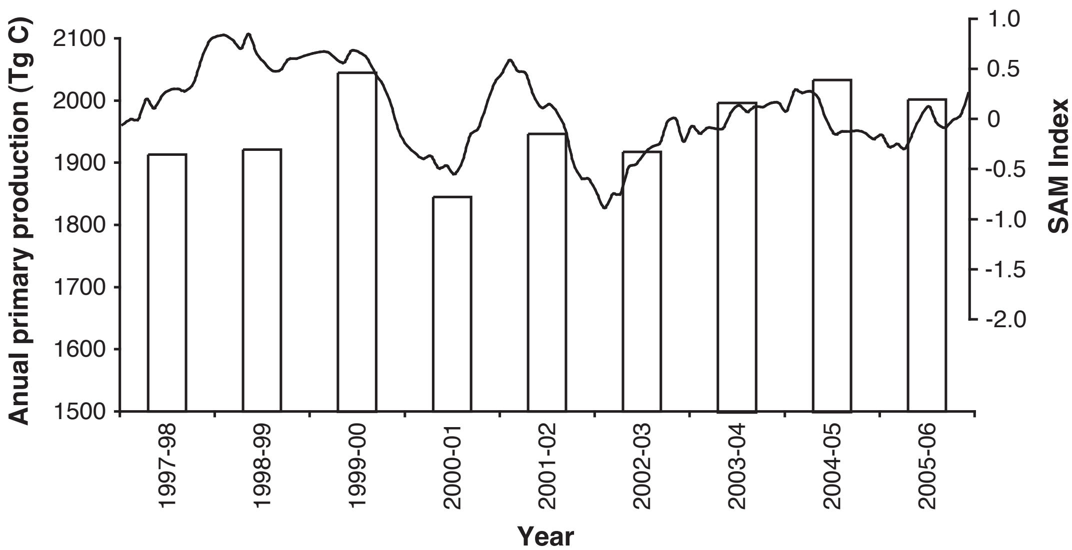
Anual primary production (Tg C)
2100
2000
1900
1800
1700
1600
1500
1.0
0.5
0
-0.5
-1.0
-1.5
-2.0
SAM Index
1997-98
1998-99
1999-00
2000-01
2001-02
2002-03
2003-04
2004-05
2005-06
Year

Figure 14

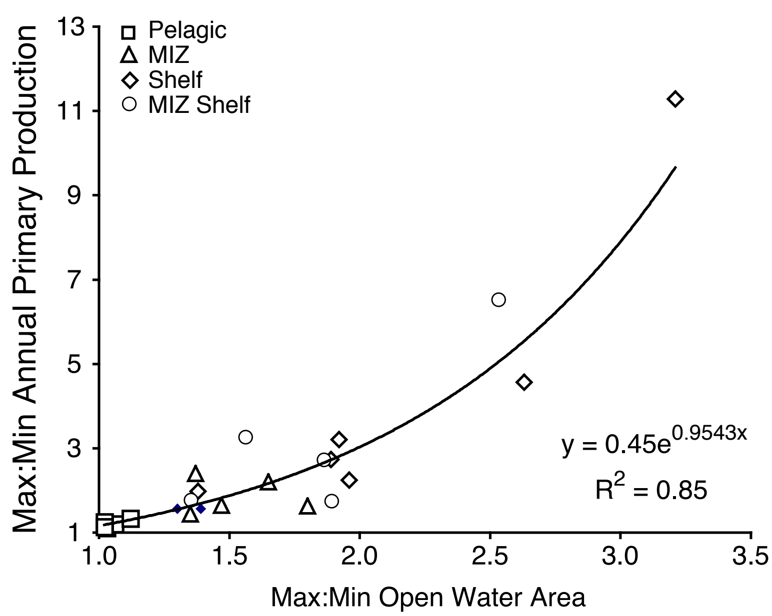
13
11
9
7
5
3
1
1.0
1.5
2.0
2.5
3.0
3.5
Pelagic
MIZ
Shelf
MIZ Shelf
y = 0.45e^0.9543x
R^2 = 0.85
Max:Min Annual Primary Production
Max:Min Open Water Area

Figure 15

Table 1. Mean Chlorophyll *a* (mg m^{-3}) in the Southern Ocean derived *in situ* and using SeaWiFS

	SeaWiFS	*In situ*
Southern Ocean	0.34	0.54
Southern Ocean (offshore waters only)	0.28	0.36
West Antarctic Peninsula (WAP)	0.53	1.91
Ross Sea	2.18	2.53
Weddell/Scotia Sea	0.62	0.92
Weddell/Scotia Sea (minus Scotia Ridge)	0.62	0.61
Prydz Bay	1.06	0.92

Table 2. Mean (Maximum) Open Water Area (10^6 km^2) by Geographic Sector and Ecological Province.

	Pelagic	MIZ	Shelf	MIZ shelf	Total
Bellingshausen-Amundsen Sea					
1997-98	7.02 (7.73)	0.19 (0.84)	0.114 (0.35)	0.074 (0.25)	7.40 (8.28)
1998-99	7.05 (7.77)	0.17 (0.63)	0.169 (0.45)	0.080 (0.21)	7.46 (8.41)
1999-00	6.86 (7.67)	0.25 (0.79)	0.136 (0.37)	0.077 (0.20)	7.32 (8.39)
2000-01	6.97 (7.70)	0.20 (0.69)	0.141 (0.33)	0.067 (0.19)	7.38 (8.22)
2001-02	6.92 (7.77)	0.22 (0.95)	0.131 (0.34)	0.074 (0.21)	7.35 (8.37)
2002-03	7.08 (7.89)	0.20 (0.68)	0.141 (0.45)	0.076 (0.20)	7.49 (8.45)
2003-04	6.94 (7.74)	0.18 (0.57)	0.145 (0.41)	0.072 (0.18)	7.34 (8.34)
2004-05	6.80 (7.74)	0.20 (0.64)	0.085 (0.23)	0.057 (0.22)	7.15 (8.24)
2005-06	7.14 (7.83)	0.18 (0.60)	0.098 (0.26)	0.068 (0.20)	7.49 (8.25)
Mean	6.97 (7.76)	0.20 (0.71)	0.129 (0.35)	0.072 (0.21)	7.37 (8.33)
SD	0.11 (0.07)	0.02 (0.12)	0.026 (0.08)	0.007 (0.02)	0.11 (0.08)
Ross Sea					
1997-98	6.91 (8.75)	0.30 (1.24)	0.060 (0.34)	0.052 (0.22)	7.32 (9.39)
1998-99	6.43 (8.73)	0.39 (1.82)	0.096 (0.45)	0.041 (0.19)	6.96 (9.60)
1999-00	6.62 (8.94)	0.38 (1.48)	0.102 (0.42)	0.042 (0.29)	7.14 (9.77)
2000-01	6.71 (8.72)	0.31 (1.16)	0.068 (0.36)	0.046 (0.19)	7.13 (9.49)
2001-02	6.81 (8.77)	0.41 (1.66)	0.099 (0.44)	0.042 (0.23)	7.36 (9.78)
2002-03	6.91 (8.86)	0.30 (1.04)	0.021 (0.14)	0.041 (0.25)	7.27 (9.36)
2003-04	7.00 (8.80)	0.34 (1.01)	0.055 (0.37)	0.050 (0.27)	7.44 (9.57)
2004-05	6.99 (9.22)	0.34 (1.52)	0.103 (0.42)	0.040 (0.21)	7.48 (9.82)
2005-06	6.98 (9.15)	0.35 (1.40)	0.105 (0.42)	0.045 (0.27)	7.48 (9.83)
Mean	6.82 (8.88)	0.35 (1.37)	0.079 (0.37)	0.044 (0.23)	7.29 (9.62)
SD	0.20 (0.19)	0.04 (0.28)	0.029 (0.10)	0.004 (0.04)	0.18 (0.18)
S. Indian					
1997-98	5.85 (7.52)	0.30 (1.65)	0.049 (0.20)	0.035 (0.13)	6.23 (7.80)
1998-99	5.76 (7.52)	0.31 (1.58)	0.032 (0.15)	0.027 (0.09)	6.14 (7.77)
1999-00	5.70 (7.45)	0.30 (1.22)	0.026 (0.14)	0.028 (0.09)	6.05 (7.72)
2000-01	5.85 (7.55)	0.28 (1.45)	0.044 (0.18)	0.031 (0.09)	6.20 (7.80)
2001-02	5.82 (7.43)	0.31 (1.46)	0.029 (0.15)	0.036 (0.10)	6.20 (7.71)
2002-03	5.96 (7.56)	0.29 (1.34)	0.048 (0.19)	0.032 (0.08)	6.33 (7.82)
2003-04	5.80 (7.56)	0.30 (1.38)	0.043 (0.19)	0.035 (0.09)	6.17 (7.83)
2004-05	5.65 (7.50)	0.30 (1.48)	0.025 (0.11)	0.031 (0.15)	6.01 (7.74)
2005-06	5.76 (7.57)	0.30 (1.60)	0.039 (0.18)	0.035 (0.12)	6.13 (7.82)
Mean	5.79 (7.52)	0.30 (1.46)	0.037 (0.16)	0.032 (0.10)	6.16 (7.78)
SD	0.09 (0.05)	0.01 (0.14)	0.010 (0.03)	0.003 (0.02)	0.10 (0.05)

Table 2. Continued.

S. W. Pacific					
1997-98	6.23 (7.01)	0.22 (0.66)	0.033 (0.15)	0.040 (0.11)	6.52 (7.30)
1998-99	6.10 (6.99)	0.23 (0.77)	0.033 (0.15)	0.039 (0.11)	6.40 (7.28)
1999-00	6.14 (7.12)	0.23 (0.70)	0.054 (0.22)	0.047 (0.18)	6.47 (7.44)
2000-01	6.27 (6.98)	0.22 (0.79)	0.026 (0.12)	0.039 (0.10)	6.55 (7.25)
2001-02	6.35 (7.15)	0.21 (0.66)	0.057 (0.24)	0.058 (0.18)	6.68 (7.50)
2002-03	6.31 (7.02)	0.19 (0.57)	0.037 (0.14)	0.042 (0.12)	6.58 (7.30)
2003-04	6.19 (7.02)	0.25 (0.66)	0.034 (0.15)	0.043 (0.10)	6.51 (7.33)
2004-05	6.28 (6.98)	0.22 (0.63)	0.035 (0.16)	0.046 (0.12)	6.58 (7.33)
2005-06	6.21 (6.99)	0.21 (0.62)	0.032 (0.13)	0.039 (0.12)	6.49 (7.28)
Mean	6.23 (7.03)	0.22 (0.67)	0.038 (0.16)	0.044 (0.12)	6.53 (7.33)
SD	0.08 (0.06)	0.01 (0.07)	0.010 (0.04)	0.006 (0.03)	0.08 (0.08)
Weddell Sea					
1997-98	6.06 (9.28)	0.46 (2.57)	0.131 (0.52)	0.067 (0.24)	6.72 (10.16)
1998-99	6.52 (9.61)	0.42 (2.50)	0.113 (0.25)	0.048 (0.15)	7.10 (10.08)
1999-00	6.47 (9.41)	0.41 (2.45)	0.115 (0.25)	0.047 (0.17)	7.04 (9.96)
2000-01	6.10 (9.07)	0.41 (1.93)	0.092 (0.31)	0.061 (0.22)	6.66 (9.73)
2001-02	6.38 (9.16)	0.48 (2.18)	0.144 (0.28)	0.045 (0.11)	7.05 (9.69)
2002-03	5.77 (8.58)	0.40 (1.94)	0.095 (0.27)	0.069 (0.27)	6.34 (9.23)
2003-04	5.88 (8.80)	0.49 (2.04)	0.092 (0.20)	0.045 (0.11)	6.50 (9.46)
2004-05	6.24 (9.27)	0.45 (2.54)	0.117 (0.26)	0.052 (0.11)	6.85 (9.77)
2005-06	6.19 (9.35)	0.46 (2.84)	0.109 (0.26)	0.061 (0.17)	6.81 (9.92)
Mean	6.18 (9.17)	0.44 (2.33)	0.112 (0.29)	0.055 (0.17)	6.79 (9.78)
SD	0.26 (0.32)	0.03 (0.32)	0.018 (0.09)	0.010 (0.06)	0.26 (0.30)
Total					
1997-98	32.07 (40.13)	1.48 (4.88)	0.39 (1.46)	0.27 (0.74)	34.20 (42.75)
1998-99	31.87 (40.56)	1.52 (5.93)	0.44 (1.42)	0.24 (0.53)	34.06 (43.05)
1999-00	31.78 (40.30)	1.57 (5.09)	0.43 (1.36)	0.24 (0.64)	34.02 (43.12)
2000-01	31.89 (39.97)	1.42 (4.57)	0.37 (1.24)	0.24 (0.62)	33.93 (42.24)
2001-02	32.28 (40.10)	1.63 (5.54)	0.46 (1.42)	0.25 (0.64)	34.63 (42.91)
2002-03	32.02 (39.67)	1.39 (4.59)	0.34 (1.06)	0.26 (0.72)	34.02 (41.89)
2003-04	31.80 (39.86)	1.55 (4.98)	0.37 (1.24)	0.24 (0.63)	33.96 (42.35)
2004-05	31.97 (40.66)	1.51 (5.57)	0.36 (1.13)	0.23 (0.58)	34.07 (42.71)
2005-06	32.27 (40.84)	1.49 (5.52)	0.38 (1.15)	0.25 (0.62)	34.40 (42.93)
Mean	31.99 (40.23)	1.51 (5.19)	0.39 (1.28)	0.25 (0.64)	34.14 (42.66)
SD	0.19 (0.39)	0.07 (0.48)	0.04 (0.14)	0.01 (0.06)	0.23 (0.41)

Table 3. Regression Coefficients for Annual Primary Production (Tg C yr^{-1}) Versus Mean Open Water Area (10^6 km^2), Annual Primary Production Versus Year, and Mean Open Water Area Versus Year by Geographic Sector and Ecological Province.

	Production vs Open water			Production vs Year			Open water vs Year		
	R^2	*p*-value	Slope	R^2	*p*-value	Slope	R^2	*p*-value	Slope
South Indian Ocean									
Pelagic	0.002	0.915	-7.683	**0.520**	**0.028**	**-0.118**	0.035	0.627	-0.006
MIZ	0.179	0.257	78.75	0.056	0.539	0.142	0.061	0.520	-0.001
Shelf	**0.687**	**0.006**	**191.8**	0.002	0.905	0.038	0.011	0.786	0.000
MIZ-shelf	**0.537**	**0.025**	**108.1**	0.005	0.861	-0.012	0.169	0.272	0.000
Total	0.005	0.859	12.33	**0.456**	**0.046**	**-4.236**	0.038	0.615	-0.007
Bellingshausen-Amundsen Sea									
Pelagic	0.064	0.512	-34.44	0.221	0.201	2.493	0.000	1.000	0.000
MIZ	**0.770**	**0.002**	**87.26**	0.005	0.863	-0.057	0.027	0.670	-0.001
Shelf	**0.542**	**0.024**	**97.22**	0.050	0.564	-0.276	0.272	0.150	-0.005
MIZ-shelf	0.096	0.418	60.89	0.007	0.832	-0.042	0.396	0.070	-0.002
Total	0.314	0.117	-65.44	0.208	0.217	2.100	0.038	0.617	-0.008
Ross Sea									
Pelagic	**0.556**	**0.021**	**112.9**	**0.491**	**0.036**	**7.612**	**0.457**	**0.045**	**0.049**
MIZ	0.369	0.083	62.67	0.085	0.447	0.424	0.002	0.906	-0.001
Shelf	**0.960**	**0.000**	**333.2**	0.002	0.906	0.169	0.010	0.795	0.001
MIZ-shelf	0.020	0.717	78.43	0.004	0.876	-0.050	0.048	0.573	0.000
Total	0.413	0.062	116.7	**0.540**	**0.024**	**8.761**	**0.552**	**0.022**	**0.049**

Table 3. Continued.

Southwest Pacific Ocean									
Pelagic	0.006	0.848	-11.73	0.079	0.463	-1.289	0.112	0.378	0.010
MIZ	0.064	0.510	52.10	0.001	0.949	-0.026	0.017	0.736	-0.001
Shelf	**0.925**	**0.000**	**208.8**	0.026	0.681	-0.132	0.014	0.766	0.000
MIZ-shelf	**0.756**	**0.002**	**168.9**	0.014	0.762	-0.052	0.016	0.747	0.000
Total	0.003	0.893	11.52	0.058	0.532	-1.519	0.103	0.399	0.009
Weddell Sea									
Pelagic	0.180	0.255	69.98	0.234	0.187	7.454	0.109	0.385	-0.031
MIZ	**0.454**	**0.047**	**112.0**	0.396	0.069	1.235	0.070	0.492	0.003
Shelf	0.334	0.103	230.4	0.248	0.173	-1.287	0.095	0.420	-0.002
MIZ-shelf	**0.543**	**0.024**	**283.4**	0.271	0.151	-0.699	0.002	0.916	0.000
Total	0.192	0.239	71.19	0.149	0.306	5.968	0.099	0.409	-0.030
Southern Ocean									
Pelagic	0.096	0.418	-100.8	0.193	0.236	9.747	0.097	0.414	0.021
MIZ	**0.635**	**0.010**	**133.6**	0.124	0.353	1.607	0.001	0.945	-0.001
Shelf	**0.755**	**0.002**	**267.3**	0.125	0.351	-1.570	0.201	0.227	-0.006
MIZ-shelf	**0.443**	**0.050**	**248.8**	0.229	0.193	-0.816	0.091	0.431	-0.001
Total	0.004	0.866	19.91	0.112	0.379	8.555	0.026	0.681	0.014

Bold denotes statistical significance at the 95% confidence level. In all cases, n=9.

Table 5. Annual Primary Production (Tg C yr^{-1}) by Geographic Sector and Ecological Province.

Bellingshausen-Amundsen Sea

	Pelagic	MIZ	Shelf	MIZ shelf	Total
1997-98	367	7.22	12.0	6.88	396
1998-99	336	5.96	16.1	5.62	367
1999-00	349	11.0	14.0	7.06	386
2000-01	357	8.57	17.3	8.12	396
2001-02	341	13.1	20.3	9.45	387
2002-03	348	8.68	16.6	7.87	384
2003-04	374	7.66	16.5	8.26	411
2004-05	376	8.55	9.08	5.27	403
2005-06	364	6.09	12.1	5.98	391
Mean	357	8.54	14.9	7.17	391
SD	14.5	2.31	3.40	1.38	12.6

Ross Sea

	Pelagic	MIZ	Shelf	MIZ shelf	Total
1997-98	410	21.1	17.0	8.78	462
1998-99	399	27.4	28.3	8.85	492
1999-00	398	24.3	33.5	7.34	486
2000-01	410	19.7	19.2	5.51	465
2001-02	417	26.4	32.5	11.3	523
2002-03	452	20.1	2.97	3.45	483
2003-04	483	22.7	18.1	8.74	548
2004-05	459	32.1	28.3	8.27	548
2005-06	426	24.6	31.2	8.28	516
Mean	428	24.3	23.4	7.84	503
SD	29.8	3.98	9.98	2.24	32.6

S. Indian

	Pelagic	MIZ	Shelf	MIZ shelf	Total
1997-98	257	11.3	8.01	3.46	288
1998-99	243	13.0	8.10	2.31	278
1999-00	273	15.8	5.36	2.37	301
2000-01	239	11.0	8.22	2.52	270
2001-02	225	12.9	3.88	2.68	252
2002-03	240	13.2	10.6	2.62	277
2003-04	241	15.3	8.64	3.03	279
2004-05	229	14.3	4.72	1.97	258
2005-06	217	12.3	8.88	3.18	249
Mean	240	13.2	7.38	2.68	272
SD	16.8	1.65	2.21	0.47	17.2

Table 6. Continued

S. W. Pacific

	Pelagic	MIZ	Shelf	MIZ shelf	Total
1997-98	288	7.14	3.12	2.06	304
1998-99	292	7.53	4.35	2.69	311
1999-00	320	14.4	8.88	4.63	352
2000-01	285	5.99	2.77	1.93	299
2001-02	298	13.0	8.38	5.29	327
2002-03	309	7.14	3.73	2.70	326
2003-04	288	9.79	3.47	2.07	307
2004-05	289	7.68	3.92	2.59	308
2005-06	281	8.64	3.93	2.45	299
Mean	295	9.03	4.73	2.94	315
SD	12.5	2.86	2.26	1.20	17.3

Weddell Sea

	Pelagic	MIZ	Shelf	MIZ shelf	Total
1997-98	364	31.1	30.3	14.9	464
1998-99	421	27.2	9.05	4.44	473
1999-00	459	31.5	12.0	4.21	519
2000-01	357	24.8	16.1	7.38	414
2001-02	390	39.1	15.7	3.46	457
2002-03	395	29.3	7.57	6.41	446
2003-04	397	33.0	6.63	2.28	451
2004-05	448	36.2	14.6	4.75	517
2005-06	477	41.0	11.6	5.33	546
Mean	412	32.6	13.7	5.90	477
SD	42.2	5.37	7.08	3.68	42.4

Total

	Pelagic	MIZ	Shelf	MIZ shelf	Total
1997-98	1704	71.9	71.0	35.8	1922
1998-99	1691	81.8	70.7	25.3	1914
1999-00	1804	98.8	77.1	26.7	2051
2000-01	1637	68.5	63.6	25.1	1830
2001-02	1665	107	83.1	34.6	1933
2002-03	1722	81.1	41.9	23.7	1890
2003-04	1781	86.9	55.9	24.5	1989
2004-05	1807	95.9	61.5	23.0	2029
2005-06	1754	88.2	70.3	26.7	1980
Mean	1729	86.7	66.1	27.3	1949
SD	60.7	12.5	12.2	4.67	70.1

Table 6. Regression Coefficients for Annual Primary Production (Tg C yr^{-1}) Versus SAM, Chl *a* versus SAM, and SST versus SAM.

	Production vs SAM			Chl *a* vs SAM			SST vs SAM		
	R^2	*p*-value	Slope	R^2	*p*-value	Slope	R^2	*p*-value	Slope
South Indian Ocean									
Pelagic	0.233	0.187	20.12	0.350	0.092	0.022	0.016	0.749	-0.051
MIZ	0.193	0.236	1.794	0.051	0.557	0.029	0.272	0.149	-0.118
Shelf	0.162	0.282	-2.205	0.010	0.795	-0.058	0.001	0.951	0.004
MIZ-shelf	0.007	0.828	-0.098	0.103	0.398	-0.041	**0.476**	**0.040**	**-0.108**
Total	0.176	0.260	17.88	0.217	0.205	0.017	0.020	0.714	-0.056
Bellingshausen-Amundsen Sea									
Pelagic	0.083	0.450	-10.40	0.002	0.918	0.001	0.187	0.245	-0.360
MIZ	0.000	0.987	0.034	0.071	0.488	-0.101	0.208	0.217	-0.066
Shelf	0.024	0.690	-1.307	0.319	0.112	-0.240	0.008	0.824	-0.023
MIZ-shelf	0.126	0.348	-1.218	0.134	0.332	-0.144	0.028	0.665	-0.026
Total	0.065	0.277	-12.70	0.016	0.743	-0.003	0.195	0.235	-0.361
Ross Sea									
Pelagic	0.198	0.230	-32.83	0.022	0.700	0.004	**0.495**	**0.021**	**-0.308**
MIZ	0.179	0.255	4.187	0.108	0.387	-0.053	0.297	0.129	-0.096
Shelf	0.409	0.063	15.82	**0.644**	**0.009**	**0.826**	0.256	0.164	-0.308
MIZ-shelf	0.320	0.111	3.144	0.236	0.185	0.387	0.209	0.215	0.059
Total	0.002	0.909	3.607	0.310	0.119	0.035	**0.726**	**0.004**	**-0.371**
Southwest Pacific Ocean									
Pelagic	0.087	0.439	9.185	0.421	0.058	0.020	**0.594**	**0.015**	**-0.393**
MIZ	0.295	0.130	3.855	0.202	0.225	0.133	0.278	0.144	-0.094
Shelf	0.284	0.139	2.995	0.268	0.153	0.202	0.020	0.714	-0.026
MIZ-shelf	0.165	0.276	1.206	0.232	0.189	0.130	0.144	0.313	-0.049
Total	0.167	0.274	17.50	0.385	0.074	0.025	**0.564**	**0.012**	**-0.400**
Weddell Sea									
Pelagic	0.183	0.250	44.80	0.005	0.854	0.006	0.032	0.111	0.057
MIZ	0.008	0.812	1.235	0.320	0.112	0.069	**0.562**	**0.020**	**0.110**
Shelf	0.002	0.915	0.701	0.016	0.741	0.091	**0.549**	**0.022**	**0.182**
MIZ-shelf	0.016	0.745	-1.154	0.032	0.642	0.118	0.023	0.697	0.214
Total	0.220	0.201	49.40	0.017	0.733	0.011	0.429	0.055	0.067
Southern Ocean									
Pelagic	0.102	0.401	48.14	0.308	0.120	0.014	**0.472**	**0.041**	**-0.247**
MIZ	0.139	0.322	11.58	0.039	0.607	0.013	0.244	0.177	-0.060
Shelf	0.408	0.064	19.29	0.343	0.096	0.155	0.103	0.399	0.023
MIZ-shelf	0.057	0.532	2.788	0.224	0.197	0.130	0.010	0.798	0.005
Total	0.305	0.123	95.98	0.428	0.055	0.020	**0.516**	**0.029**	**-0.252**

Bold denotes statistical significance at the 95% confidence level.